State of Oregon
Department of Geology and Mineral Industries
Vicki S. McConnell, State Geologist

Open-File Report O-08-06

PRELIMINARY GEOLOGIC MAP OF THE LINNTON 7.5′ QUADRANGLE, MULTNOMAH AND WASHINGTON COUNTIES, OREGON

By
Ian P. Madin[1], Lina Ma[1], and Clark A. Niewendorp[1]

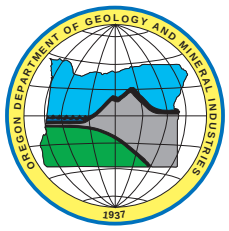

2008

[1]Oregon Department of Geology and Mineral Industries, 800 NE Oregon Street #28, Suite 965, Portland, Oregon 97232-2162

NOTICE

NO WARRANTY, EXPRESSED OR IMPLIED, IS MADE REGARDING THE ACCURACY OR UTILITY OF THE INFORMATION DESCRIBED AND/OR CONTAINED HEREIN, NOR SHALL THE ACT OF DISTRIBUTION CONSTITUTE AND SUCH WARRANTY. THIS DISCLAIMER APPLIES BOTH TO INDIVIDUAL USE OF THE DATA AND AGGREGATE USE WITH OTHER DATA. THE OREGON DEPARTMENT OF GEOLOGY AND MINERAL INDUSTRIES SHALL NOT BE HELD LIABLE FOR IMPROPER OR INCORRECT USE OF THIS INFORMATION.

Oregon Department of Geology and Mineral Industries Open-File Report O-08-06
Published in conformance with ORS 516.030

For copies of this publication or other information about Oregon's geology and natural resources, contact:

Nature of the Northwest Information Center
800 NE Oregon Street #5, Suite 177
Portland, Oregon 97232
(503) 872-2750
http://www.naturenw.org

or these DOGAMI field offices:

Baker City Field Office
1510 Campbell Street
Baker City, OR 97814-3442
Telephone (541) 523-3133
Fax (541) 523-5992

Grants Pass Field Office
5375 Monument Drive
Grants Pass, OR 97526
Telephone (541) 476-2496
Fax (541) 474-3158

For additional information:
Administrative Offices
800 NE Oregon Street #28, Suite 965
Portland, OR 97232
Telephone (971) 673-1555
Fax (971) 673-1562
http://www.oregongeology.com
http://egov.oregon.gov/DOGAMI/

TABLE OF CONTENTS

LIST OF FIGURES

LIST OF PLATES

INTRODUCTION

The Linnton 7.5′ quadrangle is located in the northern part of the Portland urban area in northwest Oregon (Figure 1). Topographically, the area is divided by the northwest-trending Tualatin Mountains (Portland Hills) the narrow, sinuous crest of which ranges in elevation from 300 to 340 m (1,000 to 1,150 ft). The northeast front of the Tualatin Mountains drops fairly steeply to near sea level along the tidally influenced lower reach of the Willamette River and is cut by numerous short, steep, northeast-trending canyons. The southwest flank of the Tualatin Mountains descends irregularly into the Tualatin Valley, reaching elevations as low as 40 m (150 ft) on the gently sloping valley floor. The southwest flank is drained by Cedar Mill, Willow, Bronson, and Rock creeks, all of which generally flow southwest in shallow, flat-bottomed valleys.

The Tualatin Mountains fork along the north edge of the map, where McCarthy Creek runs in a steep-sided, north-northwest trending canyon. Most of the higher elevations of the Tualatin Mountains, and their northeast slope, are forested parkland, private timberland, or forested rural residential land. The City of Portland occupies the northeast corner of the map, and the City of Beaverton the southwest corner, with high-density suburban development occupying most of the intervening area (Figure 2).

This map was prepared as part of a multi-year collaborative effort between the U.S. Geological Survey (USGS) and the Oregon Department of Geology and Mineral Industries (DOGAMI) to improve geologic mapping in the Portland urban area in order to better understand earthquake hazards. The Linnton quadrangle was chosen because the Portland Hills fault and Oatfield fault project into the map area from the southeast. The Linnton quadrangle also fills a gap in the detailed mapping of the Portland area between the Portland quadrangle to the southeast (Beeson and others, 1991), and the Dixie Mountain and Sauvie Island quadrangles to the northwest, which are currently being mapped by DOGAMI and USGS, respectively. In addition, detailed geologic mapping provides information about the extensive landslide hazards in the area.

This map represents a significant departure in format from previous DOGAMI geologic quadrangle maps. Thick surficial deposits of loess, Missoula Flood sediments, and colluvium mantle much of the area, landslide deposits are abundant, and bedrock exposures are rare. In the past, geologic maps of other parts of the Tualatin Mountains have largely ignored surficial deposits and have depicted inferred bedrock geology (Beeson and others, 1989) or have presented a mix of bedrock and surficial units, even though bedrock is typically buried by younger deposits (Beeson and others, 1991). For the Linnton quadrangle, we have chosen to present two maps: a bedrock map that shows only bedrock geology inferred to extend beneath surficial deposits, and a companion map that shows only surficial deposits.

During the course of this investigation, high-resolution (1 to 2-m grid size) lidar (light detection and ranging) bare-earth digital elevation maps became available, allowing a truly revolutionary view of the geomorphology of the area. The surficial geologic map is based in large part on geomorphic interpretation of the landforms imaged with lidar data.

PREVIOUS WORK

Several previous geologic maps cover all or part of the study area. The earliest complete geologic map of the area is by Trimble (1963), at a scale of 1:62,500. The area was subsequently mapped, primarily for groundwater, by Hart and Newcomb (1965) at 1:48,000 scale; the geologic units were largely derived from Trimble's earlier work. Neither earlier map differentiated the lava flows of the Columbia River Basalt. The USGS is currently working on 1:24,000-scale mapping and remapping of the adjacent Sauvie Island and Hillsboro quadrangles. DOGAMI has published maps of the adjacent Hillsboro, Portland, Beaverton, and Mount Tabor quadrangles at 1:24,000 scale (Madin, 1990, 2004) and the adjacent Dixie Mountain quadrangle (Madin and Niewendorp, 2008).

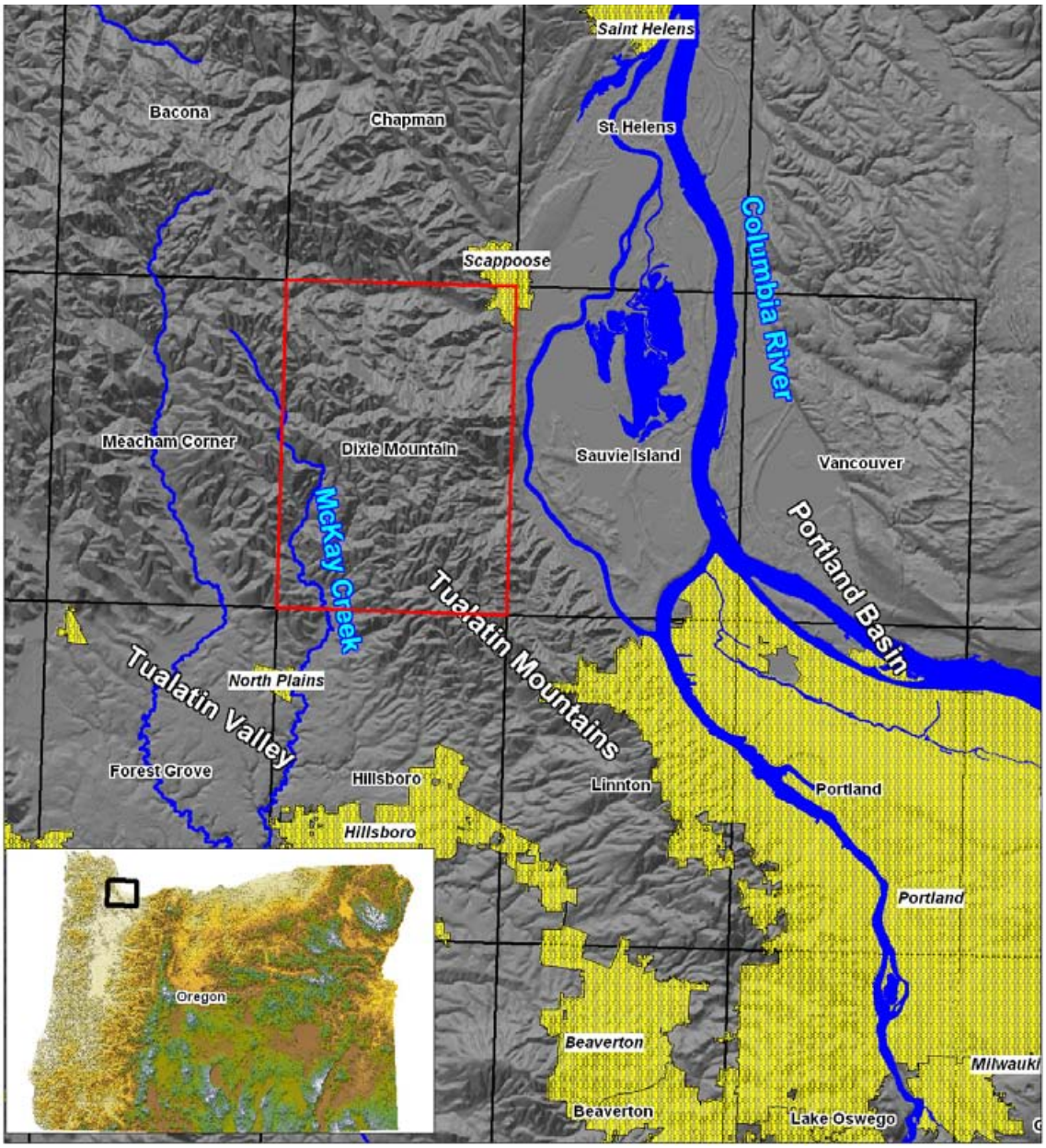

Figure 1. Shaded relief map of the Portland urban area in northwest Oregon. Grid outlines 7.5' quadrangles, labeled with quadrangle name; study area outlined in red. Yellow shading indicates area cities; selected cities are labeled in italics.

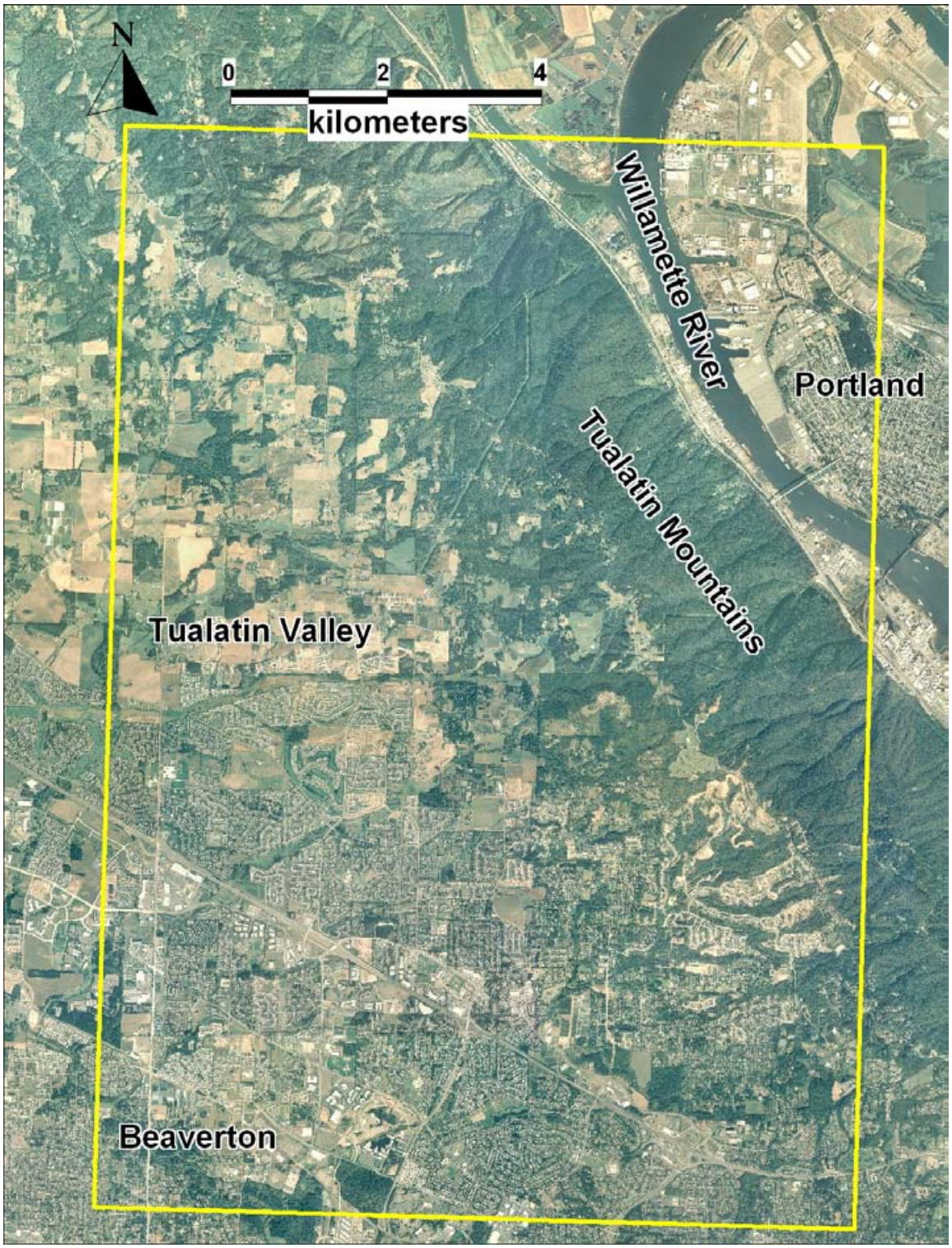

Figure 2. Orthophoto of the Linnton quadrangle showing land use patterns. Yellow box is quadrangle boundary.

METHODS

The geologic map was prepared using a variety of data, which were digitally integrated with MapInfo™ GIS software. The primary sources of data were field observations (see data map on Plate 1) in natural and man-made exposures. Over 200 observations were recorded digitally in the field using a Fujitsu Pencentra™ tablet computer running ESRI Arcpad™ software. The field observations were located using a GPS unit linked to the Pencentra, which allowed display of the GPS location on an image of the 7.5′ topographic quadrangle map and thus easy confirmation of the GPS position. The second major source of data was the logs of over 1,758 approximately located water and engineering borings in the quadrangle (data map on Plate 1). Borings were located by comparing owner, tax lot, and address information on digital images of the logs (available online through the Oregon Water Resources Department (OWRD; http://apps2.wrd.state.or.us/apps/gw/well_log/Default.aspx) with ownership, address, and tax lot information contained in the digital tax lot database for the area. Horizontal and vertical location errors were estimated for each located well and were entered in the database. A limited number of wells were located in the field with GPS; for the remainder no field check was performed.

Samples and logs from one well in the map area were interpreted and were geochemically analyzed (USGS, 2006) by Marvin Beeson and Terry Tolan. Data from this well were used to prepare the maps, and the interpreted log is included as Appendix A. A 2,400-m-deep oil exploration well is located in the quadrangle (NAD 83 UTM coordinates 518,122 m E and 5,044,628 m N). The log of this well is available online at www.oregongeology.org.

The field and boring data were integrated through analysis of high-resolution (1- to 2-m grid cell, 15-cm vertical accuracy) digital elevation models (DEMs) derived from lidar data (http://pugetsoundlidar.ess.washington.edu/) and stereo air photos. The DEMs and contour maps derived from lidar data provided a view of the true shape of the ground surface and were critical for mapping landslides and other surficial deposits. The lidar data were visualized as shaded relief, elevation color gradient, slope-shaded, and slope color gradient grids and as vector contours at 1-m intervals.

Whole-rock major and trace element geochemical analyses of approximately 74 samples of Columbia River Basalt and Boring volcanic field lavas were used to help define volcanic units. Sample numbers correspond to field station numbers and are plotted on Plate 1 with a map code for simplicity. The samples were mostly collected by the authors and analyzed by Stanley Mertzman of Franklin and Marshall College. Mertzman's methods are described in Appendix B. Several additional analyses were contributed by Ray Wells and Russell Evarts of the USGS. Those analyses were carried out at the Washington State University GeoAnalytical Lab; the methods are described by Johnson and others (1999). Geochemical data are provided in a Microsoft Excel® spreadsheet.

DESCRIPTION OF UNITS

QUATERNARY SURFICIAL MAP UNITS

With this map, we attempt to depict an accurate map of the surficial materials present in the quadrangle. This is not a map of soils, in either the engineering or the pedological sense. The map depicts the kind of material that one could expect to find in an excavation of a few meters depth. Earth materials in this environment are notoriously complex and variable in both plan view and profile, but their properties are generally of more interest than those of the underlying bedrock. The units developed from this map are from field observations and drillers' logs from water and engineering borings but are mapped on the basis of geomorphology interpreted from the lidar DEM. Surface textures, slope, and changes in slope were some of the factors used. In the end, it is important to note that very few of the more than 1,600 surficial polygons on the map are based on direct field observations; rather, the polygons are inferred from models of deposition, erosion, and mass transport informed by the geology and geomorphology.

Deposits formed by moving water and wind

Qal **alluvium (Holocene)** — gravel, sand, silt, and clay deposited in active channels and on floodplains of rivers and streams. Thin deposits of alluvium probably occur in most minor drainages, but the unit is mapped only where the lidar DEM indicates a significant width (approximately 5 m or more) of flat floodplain. The presence of a flat floodplain implies that the dominant geomorphic agent is the stream rather than the adjacent slopes. Alluvium was not mapped in streams with a ∨-shaped floor. On most streams with significant floodplains (> 15 m wide) the lidar DEM clearly indicates the location and width of the current channel, but this feature was not mapped.

The age of the alluvium in most streams is Holocene, as most of the streams at lower elevations were affected by the latest Pleistocene Missoula floods, and any alluvial deposits must postdate the floods. Above the level of the floods in the Tualatin Mountains, there is widespread evidence for rapid incision by most streams, probably in response to Holocene changes in loess accumulation rates.

Qt **terrace deposits (late Pleistocene-Holocene)** — silt and sand (?) deposits that form flat surfaces flanking the upper reaches of minor streams. The terraces appear to be remnants of a gently sloping floodplain and/or loess deposition surface that originated in a late Pleistocene landscape of much more gentle topography. This may represent a change from late Pleistocene periglacial conditions with rapid accumulation of loess to Holocene conditions with a reduction in loess deposition and re-arrangement of the lower reaches of the drainages by repeated Missoula floods. There are no field data to indicate the nature or thickness of any deposits on the terraces; they are defined exclusively on the basis of geomorphology interpreted from the lidar DEM. The terraces must be late Pleistocene to Holocene in age, as they postdate the Missoula Flood Deposits, and have been incised as much as 30 m by modern streams.

Qmf **Missoula (Bretz) flood deposits (latest Pleistocene)** — silt, sand, and minor gravel, deposited by floods caused by the repeated failure of the glacial ice dam that impounded glacial Lake Missoula (Bretz and others, 1956; Baker and Nummedal, 1978; Waitt, 1985; Allen and others, 1986). Natural exposures are rare in the map area, but a in few excavated exposures (Figure 3) flood strata are typically deposited in fining-upward beds 10 to 40 cm thick, each bed inferred to represent a single flood event. Beds are typically capped by 5- to 30-cm-thick zones of brown clay and iron oxide mottling that are interpreted to be paleosols. Beds range from massive to laminated, and in some instances are ripple cross-bedded. Extensive networks of liquefaction dikes up to 20 cm wide cut some exposures. Rare exotic (granitoids, metamorphic rocks) glacial erratics up to 1 m across are found in the fine-grained facies at elevations up to 115 m.

The flood deposits occur in two distinct settings in the quadrangle. In the Tualatin Valley the deposits are predominantly slack water silt that covers the valley floor up to 35 m thick and mantles slopes up to an elevation of 100 to 115 m.

Along the northeast foot of the Tualatin Mountains the deposits are channel deposits deposited along the margins of the main flood as it flowed through the ancestral Willamette River canyon. The channel deposits are thin discontinuous patches banked against the northeast face of the Tualatin Mountains where the deposits mantle, or form, moderately sloping benches.

The age of the flood deposits has been estimated at 19,000 to 13,000 years B.P. from tephra and carbon-14 ages from outside the map area (Mullineaux and others, 1978; Waitt, 1985; Benito and O'Connor, 2003). Recent optically stimulated luminescence (OSL) age determinations on flood silt samples collected by Ray Wells from the exposure shown in Figure 3 were reported by Shannon Mahan of the USGS (personal communication, 2007) as follows:

Figure 3. Photograph of a recent road cut in Missoula (Bretz) flood deposits (unit Qmf) along U.S. Route 26 at Cornell Road showing rhythmites. Grain size differences between silt and fine sand parts of rhythmites cause differences in moisture content, which manifest as light and dark bands. Rhythmites range from a few centimeters to a few decimeters thick, with at least 19 bands present in the photo. Stake is 4 cm wide. Note the vertical, 10-cm-wide liquefaction dike in the center of photo. Apparent dip is due to draping on slopes of a pre-flood swale.
NAD 83 UTM coordinates are 512,955 m E and 5,041,810 m N.

Sample	Location	Layer Sampled	OSL Age, ka
RW05-0913-16:45	U.S. Route 26 (bottom)	rhythmite 7	21.6 ± 2.14
RW05-0913-17:05	U.S. Route 26 (bottom)	rhythmite 12	19.7 ± 2.51
RW05-0913-17:20	U.S. Route 26 (top)	rhythmite 19	16.1 ± 1.28

OSL is optically stimulated luminescence.

Ql **primary loess (Pleistocene)** — micaceous eolian silt derived from glacial outwash transported down the Columbia River during Pleistocene glaciations. Primarily quartz and feldspar with minor mica. Typically tan, but color ranges from nearly white to brick red. Locally, the loess is indurated and jointed and weathers to angular colluvium when dry. When saturated, the loess is notoriously weak and prone to landslides and debris flows. Where deeply weathered, the loess is mottled red-brown-orange and typically develops spherical accumulations of iron oxide 1 to 3 mm in diameter (pisolites) that locally weather out and occur as a lag on the ground surface.

Lentz (1981) suggested that loess was deposited between 34 ka and 700 ka B.P. on the basis of correlations of paleosols to glacial advances and stratigraphic relations with Boring Lava and catastrophic flood deposits. Recent OSL dating of the loess by the USGS (Shannon Mahan, personal communication, 2007) resulted in the following ages:

Sample	Location	Depth	OSL Age, ka
RW05-0913-12:15	Beaverton/Portland Hills	1 m below surface	47.0 ± 6.29
RW05-0913-14:00	Skyline Road/Cornelius Pass Road	2 m below surface	38.7 ± 3.01
RW05-0913-14:30	Skyline Road/Cornelius Pass Road	5.3 m below surface	> 79

OSL is optically stimulated luminescence.

The Beaverton/Portland Hills sample is from the Linnton quadrangle (NAD 83 UTM coordinates 516,334 m E and 5,046,073 m N), and the two samples from Skyline Road/Cornelius Pass Road are within the adjacent Dixie Mountain quadrangle.

Although loess at some point blanketed nearly the entire quadrangle to a depth of tens of meters, it is mapped only as a primary, undisturbed deposit on relatively low gradient slopes and capping ridges. In the conceptual model used for the surficial map, it was assumed that during the most recent glaciation, loess accumulation was rapid, and that a thick layer of loess draped most of the topography, producing a smoothed landscape of moderate relief. When loess accumulation ceased, streams began to incise the smooth surface and mass transport began to move loess as colluvium on steepening slopes. Loess as a primary deposit is therefore generally restricted to upper slopes less than about 10 degrees. As mapped, this deposit also generally coincides with a markedly smooth appearance of the land surface as seen in the lidar DEM.

The thickness of loess encountered in wells is variable but generally ranges from 10 to 30 m.

Deposits formed by mass transport

Colluvial deposits

In this surficial map, colluvium describes a surface layer of unconsolidated sediment and organic material of variable lithology and grain size that is moving down slope under the influence of several more or less continuous processes. Colluvium generally is mapped on slopes greater than 10 degrees and in swales and valleys where there is no well-defined alluvial floodplain. Colluvium is the default surficial unit for areas where the geomorphology does not suggest the presence of any of the other defined units. The thickness of colluvium is highly variable but is typically a few meters. Colluvium is subdivided into:

Qclb **Loess and basalt fragment colluvium (Quaternary)** — colluvium composed of micaceous silt derived from loess deposits; clay and sand derived from weathered basalt; and angular pebble- to boulder-sized clasts of basalt and weathered basalt. Field observations and the genetic model suggest that this colluvium is predominantly composed of loess-derived silt near the tops of slopes adjacent to loess (unit Ql) deposits and is predominantly derived from basalt and weathered basalt near the bottom of slopes. Covers slopes and surfaces underlain by Columbia River Group Basalt bedrock and loess.

Qcm **Missoula flood silt colluvium (Quaternary)** — colluvium composed of micaceous silt and sand derived from Missoula flood deposits. This unit, along with the Missoula flood deposits, appears to be particularly susceptible to shallow landslides and debris flows. Differentiated from Missoula deposits by a typically abrupt change in geomorphology from relatively smooth flat surfaces to very irregular slopes and drainage networks with characteristically simple, steep-walled, and steep-headed gullies. Covers slopes underlain by Missoula flood sediments

Qcls **Loess and sandstone colluvium (Quaternary)** — colluvium composed of micaceous silt derived from loess deposits and clay, silt, sand, and angular to subangular pebble- to cobble-sized fragments of weathered sandstone, siltstone, and claystone derived from the Scappoose Formation. Covers slopes and surfaces underlain by loess and Scappoose Formation bedrock.

Landslide deposits

Landslide deposits are unusually abundant on the Linnton quadrangle. We mapped 620 discrete landslide deposits ranging in size from 56 m^2 to over 90 ha (900,000 m^2). Almost 4% of the area of the quadrangle is covered by landslide deposits of some form. Landslide deposits were generally mapped on the basis of geomorphology observed on lidar DEMs, a method that is remarkably effective for finding deposits of all sizes in heavily vegetated terrain (Burns, 2007; Schultz, 2004). Mapping was limited to scales of 1:4,000 or larger; closer scrutiny (the lidar DEM supports mapping at scales down to 1:1000) would probably reveal even more small landslide deposits.

All of the mapped landslide deposits are the result of one or more previous landslides, and we make no effort to map or differentiate individual landslide events. Many events were probably triggered by exceptionally heavy rainfall, seismic shaking associated with frequent prehistoric subduction zone earthquakes, or both.

The deposits have been broken down into several units on the basis of style (bedrock, surficial, or flow) age (recent, Quaternary, or Pleistocene), and composition based on the geology of the origination zone.

Qf **flow and fan deposits (latest Pleistocene-Holocene)** — mixed sand, silt, clay, gravel, and soil deposited by earthflows or debris flows, typically where minor streams and gullies enter larger valleys. These deposits are mapped entirely on the basis of subtle topography revealed by the lidar DEM (Figure 4). The deposits generally take one of two forms: fan-shaped deposits at the mouths of small gullies, which may be separated from the area where the flow originated by some distance; or lobes on slopes that are more clearly connected to an arcuate hollow upslope where the flow originated. Hollows at the heads of many drainages are suggestive of debris flow initiation zones but are mapped as such only where clearly connected to a fan deposit. Earth and debris flows typically occur during periods of high rainfall and can be triggered by human activities that concentrate runoff on slopes. These flows can move rapidly down slopes and channels and may be life-threatening. Flows and fans occur in drainages underlain by the full range of surficial materials in the area but are particularly common in drainages originating in Missoula (Bretz) flood deposits (Qmf) or Missoula flood silt colluvium (Qcm). Fan/flow deposits are not differentiated by composition because of inherent uncertainty in where the material originated.

Qlsx, Rlsx **surficial landslides (Pleistocene-Holocene)** — chaotically mixed and deformed masses of surficial material that have moved down slope. Surficial landslides are typically the result of slumps, earthflows, and composites of the two styles and involve Missoula (Bretz) flood deposits (Qmf), primary loess (Ql), loess and sandstone colluvium (Qcls), loess and basalt fragment colluvium (Qclb), and Missoula flood silt colluvium (Qcm). The surficial landslides range from a few hundred to a few thousand square meters and rarely exceed 10 ha. The deposits are typically less than 5 to10 m thick, as inferred from the height of the head scarps. The geomorphology of the typical surficial landslide deposits includes an arcuate head scarp, a hummocky surface down slope from the scarp — in many instances with minor arcuate internal scarps — and a bulging toe, although in many instances the toes have been removed by streams or are very difficult to discern.

Failure planes for surficial landslides may include paleosols in loess, contacts between loess and underlying bedrock, beds and paleosols in Missoula flood deposits, and basal contacts of colluvial deposits.

The ages of individual surficial landslide deposits are difficult to determine, so they are divided into two classes: Recent (Rlsx) deposits that visibly cut or bury roads or other man-made features, and Quaternary (Qlsx) deposits that cut or bury late Quaternary and Holocene loess, Missoula flood deposits, and colluvium.

The composition of the deposits is also differentiated on the basis of the surficial unit in which the landslide that produced the deposit originated. Qls1 is composed predominantly of Missoula (Bretz) flood deposits (Qmf), Missoula flood silt colluvium (Qcm), and colluvium derived from these units. Rls2 and Qls2 are composed predominantly of loess and basalt colluvium.

Qlbx, Pllbx **bedrock landslides (Pleistocene-Holocene)** — chaotically deformed mixes of surficial deposits and bedrock that have moved down slope. Bedrock landslide deposits are typically the result of translational block landslides, slumps, and complex combinations of the two. The deposits range in area from 200 m^2 to 94 ha, and are typically 3 to 5 ha. Bedrock landslide deposits are typically 10 to 30 m thick, as inferred from head scarp height. The geomorphology of the typical bedrock landslide deposit includes a steep arcuate head scarp, a hummocky body, and a bulging or lobate toe. Lateral scarps are commonly well developed in larger deposits. In many of the larger deposits, there is a distinct progression from discrete scarp bounded blocks near the top to a chaotic flowing mass at the toe.

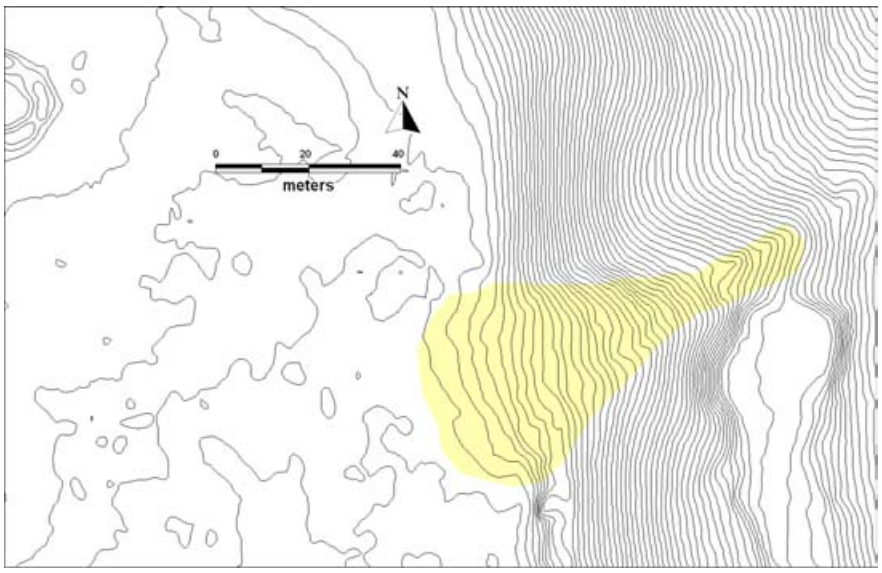

Figure 4. Fan (yellow shading) of debris flow deposits (unit Qf) at the mouth of a small gully mapped on the edge of the Rock Creek floodplain in section 1, T. 1 N., R. 1 W. Lidar derived contours are at 30-cm intervals.

Failure planes for bedrock landslides include the Vantage sedimentary horizon separating Wanapum Basalt from Grande Ronde Basalt, and the contact between the Winter Water and Ortley units of the N2 Grande Ronde.

No bedrock landslide deposits have been dated, so their ages are inferred from geomorphology and geologic relations to fall into two categories: Pleistocene (Pllb) deposits that have landslide topography smoothed due to burial by late Pleistocene loess (Ql) or by Missoula deposits (Qmf) or that are extensively incised by streams, and Quaternary (Qlb) deposits that cut or bury late Quaternary deposits and surfaces.

The composition of the all deposits is fresh and weathered Columbia River Basalt mixed with overlying surficial materials.

Other materials

af **artificial fill (Anthropocene)** — man-made deposits of mixed clay, silt, sand, gravel, debris, and rubble. The vast majority of the fill bodies mapped occur where roads intersect streams and the lidar DEM shows a body of material blocking the stream channel. The greatest volume of fill occurs in the northeast corner of the map where the banks of the Willamette River have been extensively modified and the floodplain is largely covered with one meter or more of fill to support extensive industrial development. Less common are minor dams and weirs across streams and swales. Fill associated with roads away from stream crossings and fill associated with building pads were not mapped, because the extents could not be accurately determined from the DEM.

b **bedrock exposures** — Natural or man-made surface exposures of bedrock. Commonly occur along road cuts and in the bottoms of steep canyons in the Tualatin Mountains. Many exposures in canyons inferred from lidar-based slope maps.

BEDROCK GEOLOGY MAP UNITS

Boring volcanic field rocks

Numerous small volcanoes and associated basalt flows in the Portland area have been informally known as the Boring Lava, named for exposures near the town of Boring, Oregon (Treasher, 1942). As increased geochemical and geochronological data for these volcanic rocks became available, Fleck and others (2002) proposed that the rocks be considered part of the Boring volcanic field. As used in this study, the Boring volcanic field comprises all of the late Pliocene to Pleistocene mafic volcanoes and lava flows in the greater Portland basin. Within the Linnton quadrangle, these rocks can be separated on the basis of lithology, geochemistry, age, and spatial distribution into several units described below.

Qbab **basaltic andesite of Barnes Road (Pleistocene)** — massive grey basalt flow or flows. The unit is well exposed in road cuts along Barnes Road and at the intersection of U.S. Route 26 and Oregon Route 217, and a distinct geomorphic flow front is evident (Figure 5) along the southwest edge of the unit at Cedar Hills. The unit covers approximately 330 ha on the Linnton quadrangle and an additional 65 ha on the adjacent Beaverton quadrangle. The exposed rock is relatively fresh, medium grained, and diktytaxitic, and has common 1- to 2-mm iddingsitized olivine phenocrysts. The lava is typically massive to crudely columnar jointed, with some breccia zones and voids between more massive parts. Engineering borings for St. Vincent's Hospital encountered voids that were interpreted as lava tubes (Squier, 1970).

The vent for the flow is inferred to be a roughly circular depression 200 m in diameter and 7 m deep that is located just north of Barnes Road and just east of Catlin Gabel High School (Figure 5) and occurs at the

highest and easternmost part of the flows. A limited number of well logs indicate that the thickness ranges from 30 m to 110 m near the vent, and averages 70 m. The estimated volume is approximately 0.28 km^3. Well logs indicate that over most of the its extent the lava rests on thick deposits of Hillsboro Formation and along its northwest edge overlies the basaltic andesite of Elk Point.

Geochemically, the lava is a basaltic andesite, with moderately high TiO_2 (average 1.46%) and P_2O_5 (average 0.40%) compared to other lavas in the Boring volcanic field.

No radiometric age is available for the unit, but the freshness and good preservation of flow morphology suggest that it is among the youngest flows in the area. All measured outcrops were magnetically normal.

Qbae **basaltic andesite of Elk Point (Pleistocene)—** massive grey basalt flows, scoria, and breccia. The unit is poorly exposed in road cuts along the northwest edge of Elk Point and the unnamed hill to the northwest, and at the western portal and within the western end of the Tri-County Metropolitan Transportation District of Oregon (TriMet) light rail tunnel (tunnel data provided by Ray Wells and Russell Evarts of the USGS). The unit covers approximately 1000 ha in the southeast corner of the Linnton quadrangle and several hundred additional ha on the adjacent Beaverton, Portland, and Lake Oswego quadrangles. The exposed rock is relatively fresh, medium grained, and diktytaxitic and has common 1- to 2-mm iddingsitized olivine phenocrysts. The lava is typically massive to crudely columnar jointed, with some breccia zones and voids between more massive parts. Engineering borings for the light rail tunnel encountered complexly interlayered massive lava, breccia, and scoria.

The vents for the flows are inferred to be the dome-shaped hill named Elk Point, the two unnamed conical hills just northwest of Elk Point, and Cornell Mountain, all of which retain the morphology of small cinder cones or shield volcanoes (Figure 6). Well logs indicate that the thickness ranges from 30 m to 100 m near the vents and is typically 50 to 70 m. The estimated volume is approximately 0.78 km^3. Well logs indicate that over most of the its extent the lava rests on thick deposits of Hillsboro Formation and overlies Columbia River Basalt along the eastern edge of the quadrangle where the crest of the Tualatin Mountains projects beneath the basalt of Elk Point.

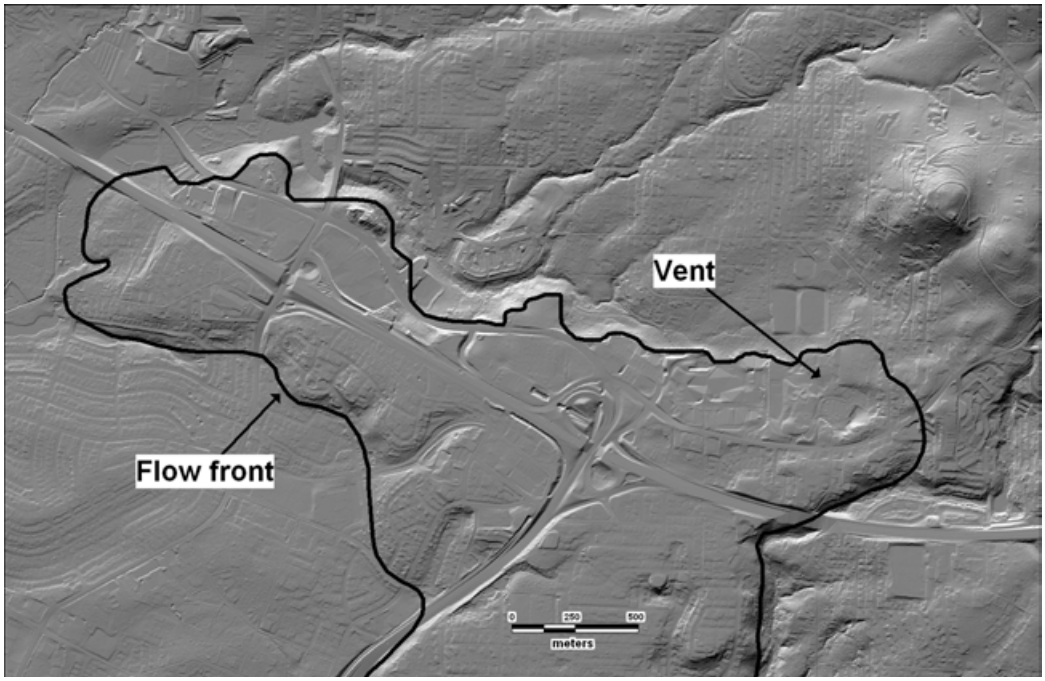

Figure 5. Shaded relief lidar DEM of the basaltic andesite of Barnes Road (unit Qbab) (outlined in heavy black) showing the distinct flow front morphology along the southwest edge, and the circular depression at the eastern edge that is the inferred vent.

Geochemically, the lavas are fairly typical Boring basaltic andesites, with average TiO_2 of 1.33 %, MgO of 6%, and P_2O_5 of 0.33%. The chemistry is indistinguishable from the basaltic andesite of Bonny Slope, but outcrop patterns and geomorphology distinguish the basaltic andesite of Elk Point.

Conrey and others (1996) report a K/Ar radiometric age of 260 ± 110 ka for magnetically normal samples from the western tunnel portal, and Fleck and others (2002) report an Ar^{40}/Ar^{39} age of 120 ± 15 ka. Other dates reported by both authors that are likely to be from the same unit range from 860 ± 40 ka to 1221 ± 110 ka, consistent with measurements of reversed magnetic polarity from some samples from the unit.

Qbk **basalt of Kaiser Road (Pleistocene)** — platy grey to grey-brown olivine basalt flow or flows. The unit is exposed in only one small area of road cut along NW Kaiser Road near the intersection with NW Wismer Road, where the unit is medium grained, diktytaxitic, platy, and moderately weathered with abundant red-brown, altered olivine phenocrysts 1 to 2 mm in diameter. The unit was also encountered in one water well logged by Beeson and Tolan (USGS, 2006; Appendix A) approximately 1,500 m southwest of the Kaiser Road exposure along West Union Road. On the basis of well data this unit probably underlies about 1,400 hectares east of Bethany and is bounded to the south by Bronson Creek and roughly to the north by Germantown Road. The likely vent is the roughly conical hill located some 1,800 m southeast of the intersection of Kaiser Road and Springville Road (Figure 7). The vent is the highest point in the area underlain by the unit and has an anomalous west-trending ridge on its west edge that suggests a dike or small canyon-filling flow. The majority of the lava appears to have flowed to the west and to the north from the vent. The thickness of the unit in wells ranges from 10 to 75 m and is typically 25 to 50 m. The estimated volume is approximately 0.5 km^3. In well logs, the unit is typically described as black where fresh, with significant thicknesses of severely weathered or cindery material commonly reported. Well logs indicate that for the most part the basalt overlies Hillsboro Formation sedimentary rocks, although at the eastern edge of the

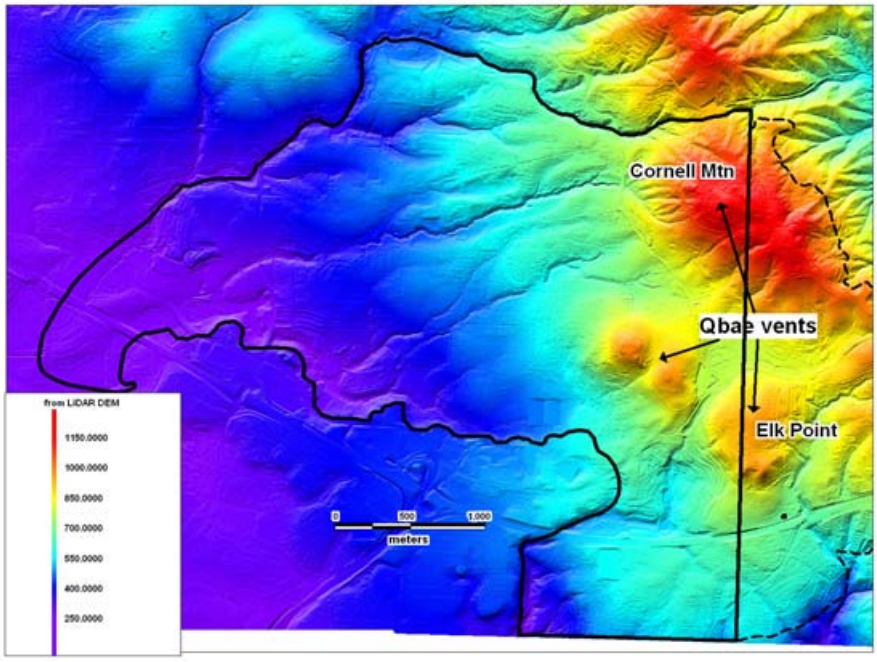

Figure 6. Color-shaded relief image derived from lidar DEM showing vents for the basalt of Elk Point (unit Qbae). Heavy black line outlines the unit on the Linnton quadrangle, heavy dashed line on Portland quadrangle. Elk Point has the shape of a small shield volcano, the two vents to the northwest of Elk Point have the shape of cinder cones, and Cornell Mountain has no distinct morphology.

extent, the Hillsboro Formation is only a few meters thick or is absent, and the basalt rests directly on weathered Columbia River Basalt.

Chemically, the unit is a basalt with unusually high TiO_2 (2.06%), MgO (8.15%), and K_2O (1.24%) compared to other Boring volcanic field rocks. Russell Evarts and Robert Fleck of the USGS (personal communication, 2007) report a provisional Ar^{40}/Ar^{39} age of 960 ± 5 ka and that the unit is magnetically reversed.

QTbb **basaltic andesite of Bonny Slope (Pliocene-Pleistocene) —** massive grey basalt flow or flows. The unit is poorly exposed in road cuts near Thompson and Salzman roads and in Cedar Mill Creek and has muted geomorphic expression (Figure 8). The unit covers approximately 830 ha between Bonny Slope and Cedar Mill and between Cedar Mill Creek and Bronson Creek. The vent for the flow is inferred to be a crudely conical hill (Figure 8), just west of Bonny Slope, and occurs at the highest and easternmost part of the extent of the flows. A limited number of well logs indicate that the thickness ranges from 10 m to 50 m and is typically 25 m. The estimated volume is approximately 0.2 km^3. Well logs indicate that over most of its extent, the basaltic andesite overlies thick deposits of Hillsboro Formation. Along the northeast edge of its extent, the basaltic andesite overlies Columbia River Basalt. Well log descriptions suggest that the lava is severely weathered through much of its thickness.

Geochemically, the lavas are fairly typical Boring basaltic andesites, with average TiO_2 of 1.33%, MgO of 6%, and P_2O_5 of 0.33%. The chemistry is indistinguishable from the basaltic andesite of Elk Point, but outcrop patterns and geomorphology distinguish the basaltic andesite of Bonny Slope.

No radiometric age is available for the unit, but the subdued geomorphology and extensive weathering suggest the age is at the older end of the range for the local Boring units. Russell Evarts (personal communication, 2008) reports that one exposure is magnetically reversed.

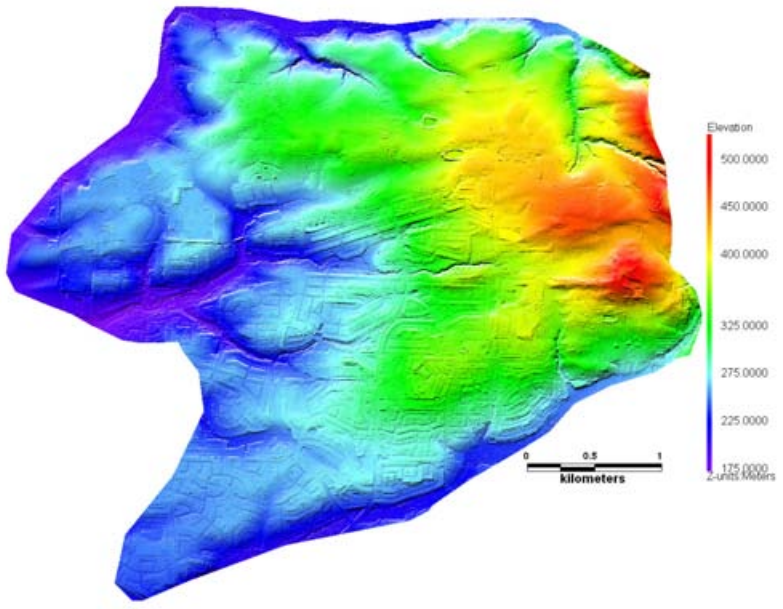

Figure 7. Color-shaded relief image derived from lidar DEM of the extent of the basalt of Kaiser Road (unit Qbk), showing the likely vent as a conical hill in the southeast corner of the image.

HIllsboro Formation

Th **Hillsboro Formation (Miocene-Pleistocene)** — fluvial sandstone, siltstone, claystone, and rare conglomerate that underlies much of the southwest half of the quadrangle. The Hillsboro Formation is everywhere buried by surficial units or Boring volcanic field rocks, and no exposures are known. In the quadrangle, the unit is known entirely from driller's logs, in which the unit is typically described as blue, green, grey, or brown silt, sand, or clay. The type section of the formation is a core hole from the adjacent Hillsboro quadrangle that was described by Wilson (1997, 1998).

The unit is banked against the southwest slope of the Tualatin Mountains, where it rests on Columbia River Basalt, and thickens to toward the southwest, reaching a maximum thickness of 268 m in the southwest corner of the quadrangle.

Wilson (1998) reports the age ranges from late Miocene to Pleistocene, on the basis of dating from diatoms, pollen, and paleomagnetism. Wilson reports, on the basis of heavy minerals and trace element geochemistry, that the unit is derived from rocks exposed in the surrounding highlands and that there is little evidence of a Columbia River sediment source for the formation. Trimble (1963), Madin (1990), and Schlicker and Deacon (1967) have called this unit Sandy River Mudstone, Sandy River Mudstone equivalent, and Helvetia Formation, respectively. The Sandy River Mudstone is a fluvial deposit of Columbia River provenance (Madin, 1990, 1994) deposited in the Portland Basin, and is clearly distinct from the Hillsboro Formation, despite occupying the same general stratigraphic position.

Troutdale Formation

Ttg **Troutdale Formation conglomerate (Miocene? and Pliocene)** — sandy pebble to cobble conglomerate preserved in several small patches deposited on Columbia River Basalt on the northeast face of the Tualatin Mountains, and underlying the entire northeast corner of the map beneath surficial deposits. The small exposures on the Tualatin Mountains consist of pebble to cobble conglomerate with a red-brown matrix of micaceous medium sand, and the clasts are typically well rounded and composed of basalt and quartz-

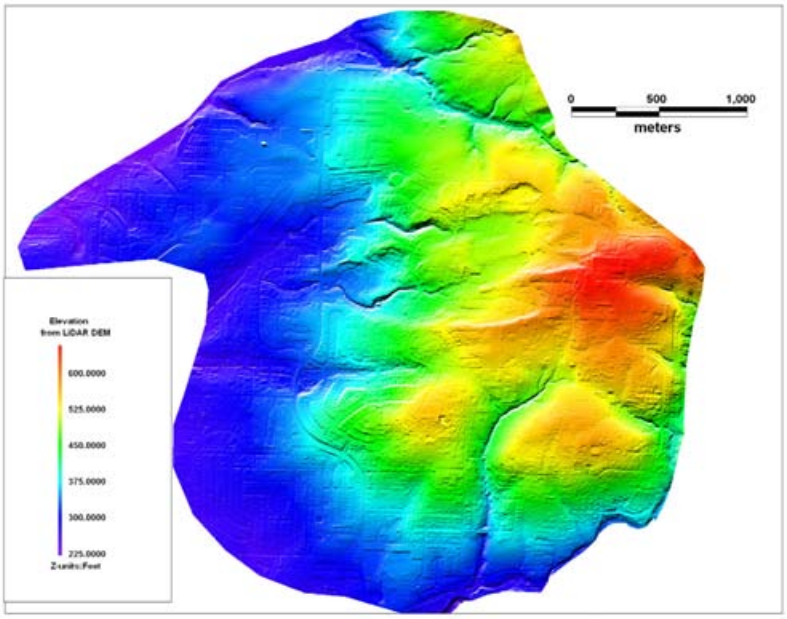

Figure 8. Color-shaded relief image derived from lidar DEM of the basaltic andesite of Bonny Slope (unit QTbb). Inferred vent is the high point along the eastern edge of polygon.

ite. The largest mapped polygon on the Tualatin Mountains is inferred from irregular topography coupled with a single borehole log that penetrated 20 m of "gravel." In the northeast corner of the quadrangle the unit makes up the bedrock north and east of the Portland Hills Fault zone and is buried under 40 to 60 m of surficial deposits. No wells penetrate the Troutdale Formation in the northeast corner of the map, but on the basis of data from Madin (1990) the thickness is probably greater than 200 m. The age of the Troutdale Formation is Miocene to Pliocene, and the provenance is predominantly from the Columbia River (Beeson and others, 1989, 1991; Madin, 1990).

Columbia River Basalt Group

Middle Miocene tholeiitic flood lavas of the Columbia River Basalt Group (CRBG) are widespread in the map area. CRBG units in the quadrangle make up but a small part of the approximately 164,000 km^2 of the Pacific Northwest underlain by hundreds of CRBG flows. Many individual flows were huge, covering thousands to tens of thousands of square kilometers, with volumes up to thousands of cubic kilometers (Tolan and others, 1989). These enormous flows erupted from vents in eastern Oregon and Washington and western Idaho, and many flowed through the Portland region on their way to the Pacific Ocean. Individual CRBG units are defined on the basis of stratigraphic position, geochemistry, magnetic polarity, and petrography following the work of Swanson and others (1979), Reidel and others (1989), and Beeson and others (1985, 1989). Recent mapping by Evarts (2004) of the nearby St. Helens quadrangle has helped refine the local stratigraphy on the basis of geochemistry.

CRBG units exposed in the map area include the Sand Hollow unit of the Frenchman Springs Member of the Wanapum Basalt. The Sentinel Bluffs Member of the Grande Ronde Basalt (Reidel, 2005) and the basalt of Winter Water and basalt of Ortley are exposed. The basalt of Wapshilla Ridge is reported from a single borehole (USGS, 2006; Appendix A, WASH 330 log).

The Barber well, a 2,400-m-deep oil exploration well, penetrated 263 m of Columbia River Basalt.

Throughout much of the map area, CRBG lavas of all units are profoundly weathered to a depth of several meters, and fresh material is found only in deep road cuts, in very rare natural exposures at the bottoms of steep canyons, and as core-stones preserved in otherwise profoundly weathered sections. Water wells typically describe as much as 20 m of "brown sandstone" in the weathered basalt horizon, and indeed the weathered material resembles a light brown or tan sandstone. Although the rock is now composed entirely of clays, relict igneous textures can commonly be seen.

Several factors severely limit the detail and accuracy with which the CRBG units can be mapped in the Linnton quadrangle.

- Due to the thickness of the surficial deposits, bedrock exposures of any kind are exceedingly rare.
- Most exposures are so weathered that only the most immobile elements remain.
- Chemical differences between some units are so subtle that even fresh basalt can be difficult to positively assign to the correct unit.
- Individual chemical flow units are typically 30 to 100 m thick, placing severe constraints on the degree of stratigraphic resolution that can be achieved.

Wanapum Basalt

Frenchman Springs Member

Twfs **basalt of Sand Hollow (middle Miocene)** — thick flow or flows of plagioclase phyric basalt. The basalt of Sand Hollow is inferred to cap a ridge in the far northwest corner of the quadrangle and was exposed only in construction excavations on the downthrown side of the Oatfield fault near the center of the quadrangle. The inferred presence in the northeast corner of the Linnton

quadrangle is projected from the adjacent Dixie Mountain quadrangle (Madin and Niewendorp, 2008).

The lava is typically black where fresh, weathering to dark grey or greenish grey. Plagioclase phenocrysts up to 2 cm in length occur sparsely in some flows.

The basalt of Sand Hollow overlies the Sentinel Bluffs Member of the Grande Ronde Basalt and is overlain only by surficial deposits.

Geochemical analysis of a single sample from the quadrangle defines the lava as a high-iron basalt, averaging 51% SiO_2, 14% FeO, 3.1% TiO_2, 3.3% MgO, and 0.62% P_2O_5. The basalt of Sand Hollow is distinguished from the underlying Grande Ronde Basalt by lower SiO_2 and higher TiO_2 and P_2O_5.

The age of the basalt of Sand Hollow is middle Miocene from a K-Ar date of 15.3 Ma reported by Beeson and others (1985).

The maximum thickness of the unit inferred for the map area is approximately 20 m.

Grande Ronde Basalt

Member of Sentinel Bluffs

Tgsb **Member of Sentinel Bluffs (middle Miocene)** — black basalt flows with sparse plagioclase phenocrysts. The Sentinel Bluffs Member is widely exposed in the northeast half of the map, where the basalt caps ridges near the crest of the Tualatin Mountains. The Member of Sentinel Bluffs overlies the basalt of Winter Water of the Grande Ronde Basalt Group.

The lava is typically dark gray or black where fresh, weathering to grayish brown. Sparse plagioclase phenocrysts up to 10 mm occur. The flows typically are blocky to platy jointed and are typically highly vesicular near the flow tops with horizontal bands of flattened vesicles and vugs. The lava weathers to form rounded core stones up to 0.5 m in diameter. Geochemically, samples of the Member of Sentinel Bluffs from the quadrangle are basaltic andesite, averaging 54% SiO_2, 10% FeO, 2% TiO_2, 4.4% MgO, and 0.34% P_2O_5. Geochemically analyzed samples are plotted on the map; complete analytical data are provided in the Excel spreadsheet.

Flows of the Sentinel Bluffs Member are part of the N2 magnetostratigraphic unit of the Grande Ronde Basalt (Swanson and others, 1979) and display normal remnant paleomagnetism. The flows are distinguished from the underlying basalt of Winter Water by their higher MgO, lower TiO_2, and higher Rb, Ni, and Cr, and from the overlying basalt of Sand Hollow by higher SiO_2, lower TiO_2 and higher MgO.

The age of the Member of Sentinel Bluffs is middle Miocene, with a reported $^{40}Ar/^{39}Ar$ date of approximately 15.6 Ma for the youngest flows of this unit on the Columbia Plateau (Long and Duncan, 1982).

The typical thickness of the unit in the map area is approximately 40 m.

Member of Winter Water

Tgww **basalt of Winter Water (middle Miocene)** — several thick flows of fine-grained grey basaltic andesite. The basalt of Winter Water is widely exposed in the northeast half of the quadrangle, where it makes up most of the lower slopes on the southwest side of the Tualatin Mountains and the bottoms of canyons on the northeast side. The basalt of Winter Water overlies the basalt of Ortley and is overlain by the Sentinel Bluffs Member. The basalt is glassy to fine grained and phyric to abundantly phyric with small (< 3 mm) plagioclase glomerocrysts that often display a distinctive radial habit. Outcrops of the basalt of Winter Water typically display columnar joint-

ing, with well developed 1- to 2-m diameter columns common in exposures along U.S. Route 30 on the northeast side of the Tualatin Mountains. Some flows also display strong platy jointing.

Geochemically, the basalt of Winter Water is a basaltic andesite, averaging 56.4% SiO_2, 10.5% FeO, 2.11% TiO_2, 3.5% MgO, and 0.36% P_2O_5. It is distinguished from the overlying Sentinel Bluffs Member by the abundance of phenocrysts, and by higher TiO_2 and lower MgO, and from the underlying basalt of Ortley by higher TiO_2 and the presence of phenocrysts. The uppermost flow is chemically somewhat distinct, with higher MgO (3.9%).

Flows of the basalt of Winter Water are part of the N2 magnetostratigraphic unit of the Grande Ronde Basalt (Swanson and others, 1979) and display normal remnant paleomagnetism.

The age of the basalt of Winter Water is middle Miocene on the basis of the basalt's stratigraphic position directly below the 15.6 Ma Sentinel Bluffs Member.

Member of Ortley

Tgo **basalt of Ortley (middle Miocene)** — several thick flows of fine-grained black basaltic andesite. The basalt of Ortley is exposed in the quadrangle only in canyon bottoms in the northeast corner of the Tualatin Mountains. The basalt of Ortley overlies the Scappoose Formation and is overlain by the basalt of Winter Water. The basalt is glassy to fine grained and aphyric and commonly displays entablature jointing.

Geochemically, the basalt of Ortley is a basaltic andesite, averaging 56.5% SiO_2, 10.5% FeO, 1.96% TiO_2, 3.5% MgO, and 0.33% P_2O_5. It is distinguished from the overlying basalt of Winter Water by the lack of phenocrysts and by slightly lower TiO_2.

Flows of the basalt of Ortley are part of the N2 magnetostratigraphic unit of the Grande Ronde Basalt (Swanson and others, 1979) and display normal remnant paleomagnetism.

The age of the basalt of Ortley is middle Miocene based on the basalt's stratigraphic position below the basalt of Winter Water and the 15.6 Ma Sentinel Bluffs Member.

Scappoose Formation

Ts **Scappoose Formation (Miocene?)** — marine sandstone, siltstone, and claystone. Scappoose Formation rocks are poorly exposed in a small window along the upthrown side of the Oatfield fault on the southwest side of the Tualatin Mountains near the center of the quadrangle. The only exposure was in a foundation excavation, where the Scappoose Formation consisted of several meters of tan to yellow-brown medium-grained micaceous arkosic sandstone with interbeds several centimeters thick of tan or white siltstone and tuffaceous siltstone, and 1-cm-thick lenses of bivalve and gastropod shell fragments. The sandstone is moderately to poorly bedded and well sorted. Several nearby water wells (MULT 403, MULT 58786) penetrate up to 50 m of "grey sandstone" beneath Columbia River Basalt, and the Barber oil exploration well penetrated several hundred meters of sedimentary rocks beneath the Columbia River Basalt, which was assigned in the well log to the Pittsburgh Bluff Formation.

Warren and others (1945) give an age for the Scappoose Formation of late Oligocene to middle Miocene on the basis of fossils and Columbia River Basalt clast conglomerate in the upper parts of the formation. In the map area the unit is likely to be all Miocene to middle Miocene, based on stratigraphic position beneath the Columbia River Basalt.

STRUCTURE

The main structure in the Linnton quadrangle is the northwest-trending Tualatin Mountains Anticline, which is truncated on the northeast by the Portland Hills fault and on the southwest by the Oatfield fault. No attitudes measured on bedding planes are available to define the anticline, but its presence is inferred from the outcrop pattern of Columbia River Basalt Group flows and the topography. Dips on both limbs are inferred to be 3 to 10 degrees, and excellent exposures in a quarry on the adjacent Sauvie Island quadrangle show a progressive steepening of strata from nearly flat at the crest of the anticline to about 13° NE dip adjacent to the Portland Hills fault. The narrow crest of the Portland Hills is distinctly sinuous in plan with a wavelength of about 5 km, and the Tualatin Mountains Anticline is also inferred to be sinuous.

The Portland Hills fault trends northwest along the northeast foot of the Tualatin Mountains and has been mapped extending tens of kilometers to the southeast across the Portland and Lake Oswego quadrangles. The location of the fault is inferred to be at the sharp break in slope where the steep slopes of the mountains intersect the relatively flat Willamette River floodplain. Engineering borings from the floodplain area on the southwest bank of the river encounter a flat basalt surface at depths of 15 to 30 m. This stratigraphic level of this surface has been identified in borings just off the east side of the map as the Wanapum-Grand Ronde contact, and off the north edge of the map as basalt of Winter Water. These observations limit the possible vertical separation of the Columbia River Basalt Group flows across the Portland Hills fault to a several tens of meters and probably to no more than 100 m. The exact location of the trace, the dip, and the sense of slip of the Portland Hills fault are unknown.

The Portland Harbor fault parallels the Portland Hills fault and is inferred to run beneath the channel of the Willamette River, where a small number of engineering borings indicate that the buried basalt surface that underlies the southwest bank of the river is truncated and that the basalt is down dropped out of the depth range of any borings. The vertical separation is inferred to be at least 50 m, northeast side down. The exact location of the trace, the dip, and the sense of slip of the Portland Harbor fault are unknown.

The East Bank fault parallels the Portland Harbor fault and is inferred to extend across the northeast corner of the map from observations on the adjacent Portland quadrangle. The sense of offset of the East Bank fault was shown as southwest side down by Madin (1990), Beeson and others (1991), and Blakely and others (1995); Blakely and others modeled the fault as a reverse fault. There is no direct evidence of the fault on the Linnton quadrangle other than the aeromagnetic lineament described by Blakely and others (1995).

The Oatfield fault trends northwest along the southwest side of the Tualatin Mountains anticline and extends for several kilometers to the southeast across the Lake Oswego and Gladstone quadrangles (Beeson and others, 1989; Madin, 1990, 2004). The trace of the Oatfield fault is everywhere buried by surficial deposits and Boring volcanic field rocks and its location is inferred from outcrop patterns and boring data. The stratigraphic separation across the Oatfield fault is substantial, juxtaposing the bottom of the local Columbia River Basalt Group section and underlying Scappoose Formation against the Wanapum Basalt at the top of the local CRBG section.

The offset is estimated at 400 to 600 m. The dip of the fault is unknown.

The Germantown Road fault trends east-west across the west-central part of the map. The trace of the fault is everywhere buried by surficial deposits or Boring volcanic field rocks, but the fault is inferred from outcrop patterns and boring logs. The offset of the fault is down to the south at least 50 m and may be as much as 100 m. The dip is unknown.

Another minor east-west trending fault cuts across the crest of the Tualatin Mountains near the southeast corner of the map and offsets the top of the Columbia River Basalt down to the south 100 to 150 m.

Acknowledgements

Research supported by the U.S. Geological Survey (USGS), Department of the Interior, under USGS award 03HQAG0013. The views and conclusions contained in this document are those of the authors and should not be interpreted as necessarily representing the official policies, either expressed or implied, of the U.S. Government.

REFERENCES

Allen, J. E., Burns, M., and Sargent, S. C., 1986, Cataclysms on the Columbia: Portland, Oreg., Timber Press, 211 p.

Baker, V. R., and Nummedal, D., eds., 1978, The Channeled Scabland: Washington, D.C., National Aeronautics and Space Administration, 186 p.

Beeson, M. H., Fecht, K. R., Reidel, S. P., and Tolan, T. L., 1985, Regional correlations within the Frenchman Springs Member of the Columbia River Basalt Group: New insights into the middle Miocene tectonics of northwestern Oregon: Oregon Geology, v. 47, no. 88, p. 87–96.

Beeson, M. H., Tolan, T. L., and Madin, I. P., 1989, Geologic map of the Lake Oswego quadrangle, Clackamas, Multnomah, and Washington counties, Oregon: Oregon Department of Geology and Mineral Industries Geologic Map Series GMS-59.

Beeson, M. H., Tolan, T. L., and Madin, I. P., 1991, Geologic map of the Portland quadrangle, Multnomah and Washington counties, Oregon: Oregon Department of Geology and Mineral Industries Geologic Map Series GMS-75.

Benito, G., and O'Connor, J. E., 2003, Number and size of last-glacial Missoula floods in the Columbia River valley between the Pasco Basin, Washington, and Portland, Oregon: Geological Society of America Bulletin, v. 115, no. 5, p. 624–638.

Blakely, R. J., Wells, R. E., Yelin, T. S., Madin, I. P., and Beeson, M. H., 1995, Tectonic setting of the Portland-Vancouver area, Oregon and Washington: Constraints from low altitude aeromagnetic data: Geological Society of America Bulletin, v. 107, no. 9, p. 1051–1062.

Bretz, J. H., Smith, H. T. U., and Neff, G. E., 1956, Channeled Scabland of Washington: New data and interpretations: Geological Society of America Bulletin, v. 67, no. 8, p. 957–1049.

Burns, W. J., 2007, Comparison of remote sensing datasets for the establishment of a landslide mapping protocol in Oregon, *in* Schaefer, V. R., Schuster, R. L., and Turner, A. K., eds., 1st North American Landslide Conference, Vail, Colo., June 3–8, 2007, Proceedings: AEG Special Publication No. 23, p. 335–345.

Conrey, R. M., Uto, K., Uchiumi, S., Beeson, M. H., Madin, I. P., Tolan, T. L., and Swanson, D. A., 1996, Potassium-argon ages of Boring Lava, northwest Oregon and southwest Washington: Isochron West, no. 63, p. 3–9.

Evarts, R. C., 2004, Geologic map of the Saint Helens quadrangle, Columbia County, Oregon, and Clark and Cowlitz counties, Washington: U.S. Geological Survey Scientific Investigations Map 2834.

Fleck, R. J., Evarts, R. C., Hagstrum, J. T., and Valentine, M. J., 2002, The Boring Volcanic Field of the Portland, Oregon area—geochronology and neotectonic significance: Geological Society of America Abstracts with Program, v. 33, no. 5, p. 33–34.

Hart, D. H., and Newcomb, R. C., 1965, Geology and ground water of the Tualatin Valley, Oregon: U.S. Geological Survey Water Supply Paper 1697.

Houston, R., 1997, Bedrock geology of the Bacona 7.5 minute quadrangle, Columbia County, Oregon: Corvallis, Oreg., Oregon State University, B.S. thesis, 36 p., 3 pls.

Johnson, D. M., Hooper P. R., and Conrey, R. M., 1999, XRF analysis of rocks and minerals for major and trace elements on a single low dilution Li-tetraborate fused bead: Advances in X-ray Analysis, v. 41, p. 843–867.

Kelty, K. B., 1981, Stratigraphy, lithofacies and environment of deposition of the Scappoose Formation in central Columbia County, Oregon: Portland, Oreg., Portland State University, M.S. thesis.

Lentz, R. T., 1981, The petrology and stratigraphy of the Portland Hills Silt — a Pacific Northwest loess: Oregon Geology, v. 43, no. 1, p. 3–10.

Long, P. E., and Duncan, R. A., 1982, $^{40}AR/^{39}AR$ ages of Columbia River Basalt from deep boreholes south Central Washington [abs]: Alaska Science Conference, 33rd, Fairbanks, Alaska, Proceedings, p. 119.

Madin, I. P., 1990, Earthquake-hazard geology maps of the Portland metropolitan area: Oregon Department of Geology and Mineral Industries Open-File Report O-90-2.

Madin, I. P., 1994, Geologic map of the Damascus quadrangle, Clackamas and Multnomah counties, Oregon: Oregon Department of Geology and Mineral Industries Geologic Map Series GMS-60.

Madin, I. P., 2004, Geologic mapping and database for Portland area fault studies, final technical report: Oregon Department of Geology Open-File Report O-04-02, 18 p.

Madin, I. P., and Niewendorp, C. A., 2008, Preliminary geologic map of the Dixie Mountain 7.5′ quadrangle, Columbia, Multnomah, and Washington counties, Oregon: Oregon Department of Geology and Mineral Industries Open-File Report O-08-07, 43 p.

Mullineaux, D. R., Wilcox, R. E., Ebaugh, W. R., Fryxell, R., and Rubin, M., 1978, Age of the last major scabland flood of the Columbia Plateau in eastern Washington: Quaternary Research, v. 10, no. 2, p. 171–180.

Reidel, S. P., 2005, A lava flow without a source: The Cohassett flow and its compositional components, Sentinel Bluffs Member, Columbia River Basalt Group: Journal of Geology, v. 113, p. 1–21.

Reidel, S. P., Tolan, T. L., Hooper, P. R., Beeson, M. H., Fecht, K. R., Bentley, R. D., and Anderson, J. L., 1989, The Grande Ronde Basalt, Columbia River Basalt Group; Stratigraphic descriptions and correlations in Washington, Oregon, and Idaho, *in* Reidel, S. P., and Hooper, P. R., eds., Volcanism and tectonism in the Columbia River Flood-Basalt Province: Geological Society of America Special Paper 239, p. 21–53.

Schlicker, H. G., and Deacon, R. J., 1967, Engineering geology of the Tualatin Valley region, Oregon: Oregon Department of Geology and Mineral Industries Bulletin 60, 103 p., 4 pls.

Schlicker, H. G., and Finlayson, C. T., 1979, Geology and geologic hazards of northwest Clackamas County, Oregon: Oregon Department of Geology and Mineral Industries Bulletin 99, 79 p., 10 pls.

Schulz, W. H., 2004, Landslides mapped using LIDAR imagery, Seattle, Washington: U.S. Geological Survey Open-File Report 2004-1396, 11 p., 1 plate.

Squier, L. R., 1970, Lava tubes cause foundation design change: Civil Engineering, A.S.C.E., v. 40, no. 8, p. 61–62.

Swanson, D. A., Wright, T. L., Hooper, P. R., and Bentley, R. D., 1979, Revisions in stratigraphic nomenclature of the Columbia River Basalt Group: U.S. Geological Survey Bulletin 1457-G, 59 p.

Tolan, T. L., Reidel, S.P., Beeson, M. H., Anderson, J. L., Fecht, K. R., and Swanson. D. A., 1989, Revisions to the estimates of the areal extent and volume of the Columbia River Basalt Group, *in* Reidel, S. P., and Hooper, P. R., eds., Volcanism and tectonism in the Columbia River Flood-Basalt Province: Geological Society of America Special Paper 239, p. 1–20.

Treasher, R. C., 1942, Geologic history of the Portland area: Oregon Department of Geology and Mineral Industries Short Paper 7, 17 p., 1 pl.

Trimble, D. E., 1963, Geology of Portland, Oregon, and adjacent areas: U.S. Geological Survey Bulletin 1119, 119 p.

U.S. Geological Survey, 2006, Columbia River Basalt Stratigraphy in Oregon: http://or.water.usgs.gov/projs_dir/crbg/, accessed October 6, 2006.

Waitt, R. B., 1985, Case for periodic, colossal jokulhlaups from Pleistocene glacial Lake Missoula: Geological Society of America Bulletin, v. 96, no. 10, p. 1271–1286.

Warren, W. C., Grivetti, R. M., and Norbisrath, H., 1945, Geology of northwest Oregon west of the Willamette River and north of latitude 45 degrees 15 minutes: U.S. Geological Survey Oil and Gas Investigation Preliminary Map 42.

Wilson, D. C., 1997, Post Middle Miocene Geologic History of the Tualatin Basin, Oregon, with hydrogeologic implications: Portland, Oreg., Portland State University, Ph.D. dissertation.

Wilson, D. C., 1998, Post Middle Miocene geologic evolution of the Tualatin Basin, Oregon: Oregon Geology, v. 60, no. 5, p. 99–116..

APPENDIX A: WELLS PENETRATING THE COLUMBIA RIVER BASALT IN THE LINNTON 7.5′ QUADRANGLE

This appendix contains .pdf files depicting the location (*_location.pdf) and geologic interpretation of wells (*_geol.pdf) that penetrated a significant section of Columbia River Basalt. The well logs and cuttings were analyzed and interpreted by Marvin Beeson and Terry Tolan and are available at the USGS website http://or.water.usgs.gov/projs_dir/crbg/index.html. The website has additional data including geochemical analyses that are not presented here. The wells in this appendix occur on or near the Linnton quadrangle and were used to help prepare the map.

ODOT TB801:

Location map: http://or.water.usgs.gov/projs_dir/crbg/data/wells/odot_tb801/odot_tb801_loca.pdf
Geologic log: http://or.water.usgs.gov/projs_dir/crbg/data/wells/odot_tb801/odot_tb801_geol.pdf

WASH330:

Location map: http://or.water.usgs.gov/projs_dir/crbg/data/wells/wash___330/wash___330_loca.pdf
Geologic log: http://or.water.usgs.gov/projs_dir/crbg/data/wells/wash___330/wash___330_geol.pdf

WASH 886:

Location map: http://or.water.usgs.gov/projs_dir/crbg/data/wells/wash___886/wash___886_loca.pdf
Geologic log: http://or.water.usgs.gov/projs_dir/crbg/data/wells/wash___886/wash___886_geol.pdf

Location Map For Site ODOT TB801

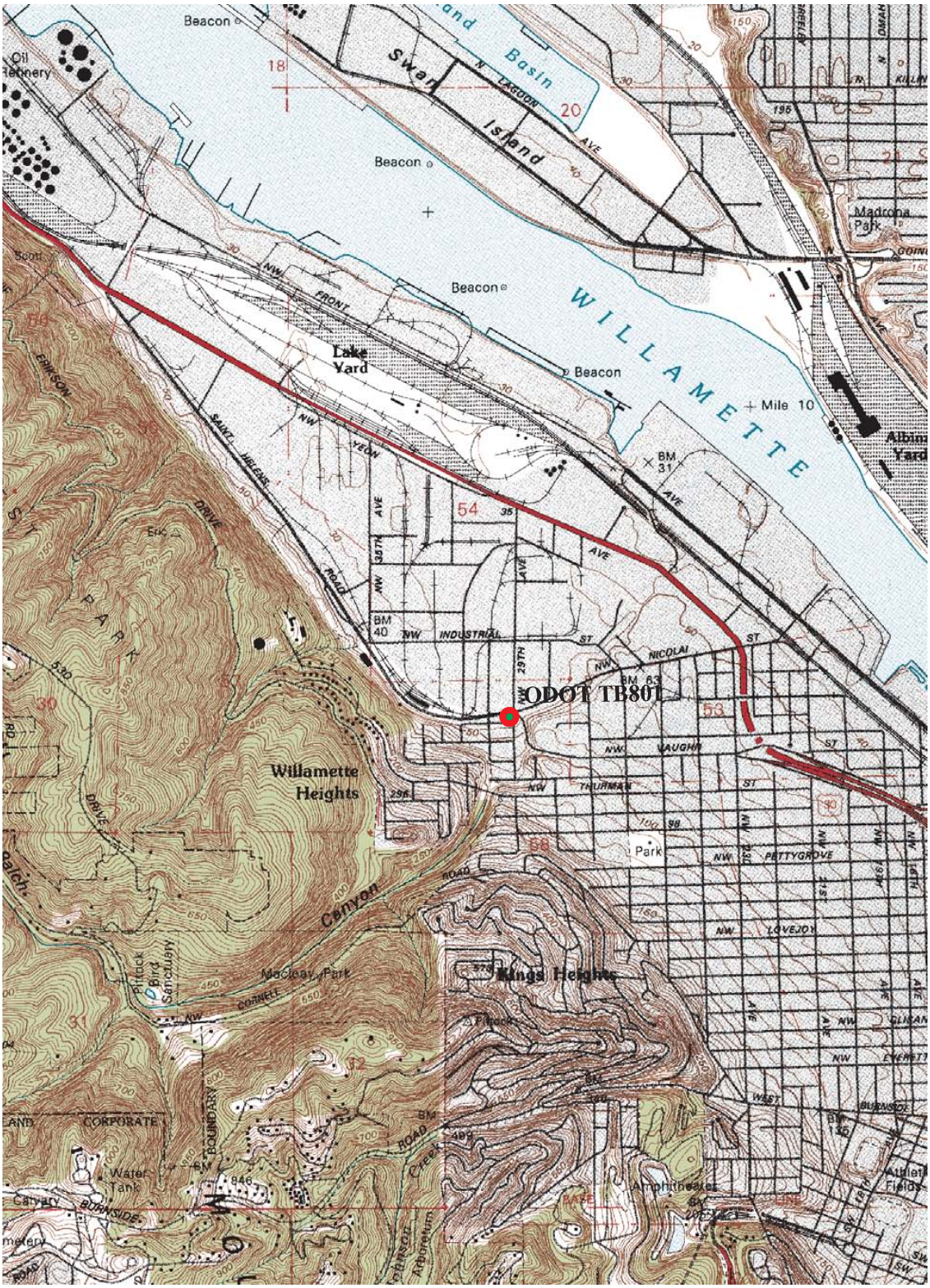

Geologic Log For Site ODOT TB801

NWIS Site ID: 453219122423601
OWRD Log ID: ODOT TB801
Well location: 01N/01E-29DBC
Depth drilled, in feet below land surface: 250
Land surface altitude, in feet above Nation Geodetic Vertical Datum of 1929: 40

Logged by: M. H. Beeson
Date drilled: 02/00/1992

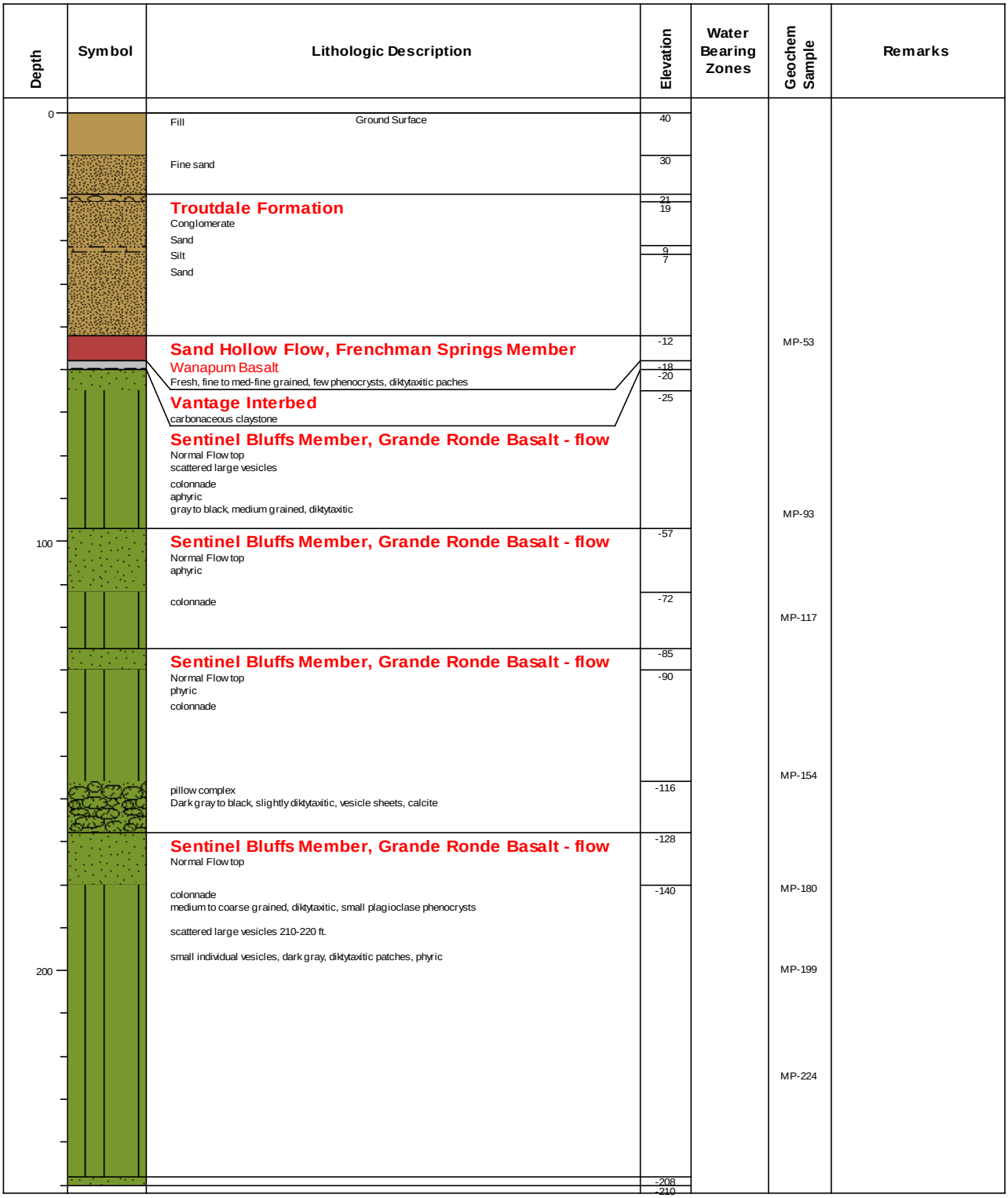

Location Map For Site WASH 330

NWIS Site ID: 453302122504101

Well location: 01N/01W-20CCC1

OWRD Log ID: WASH 330

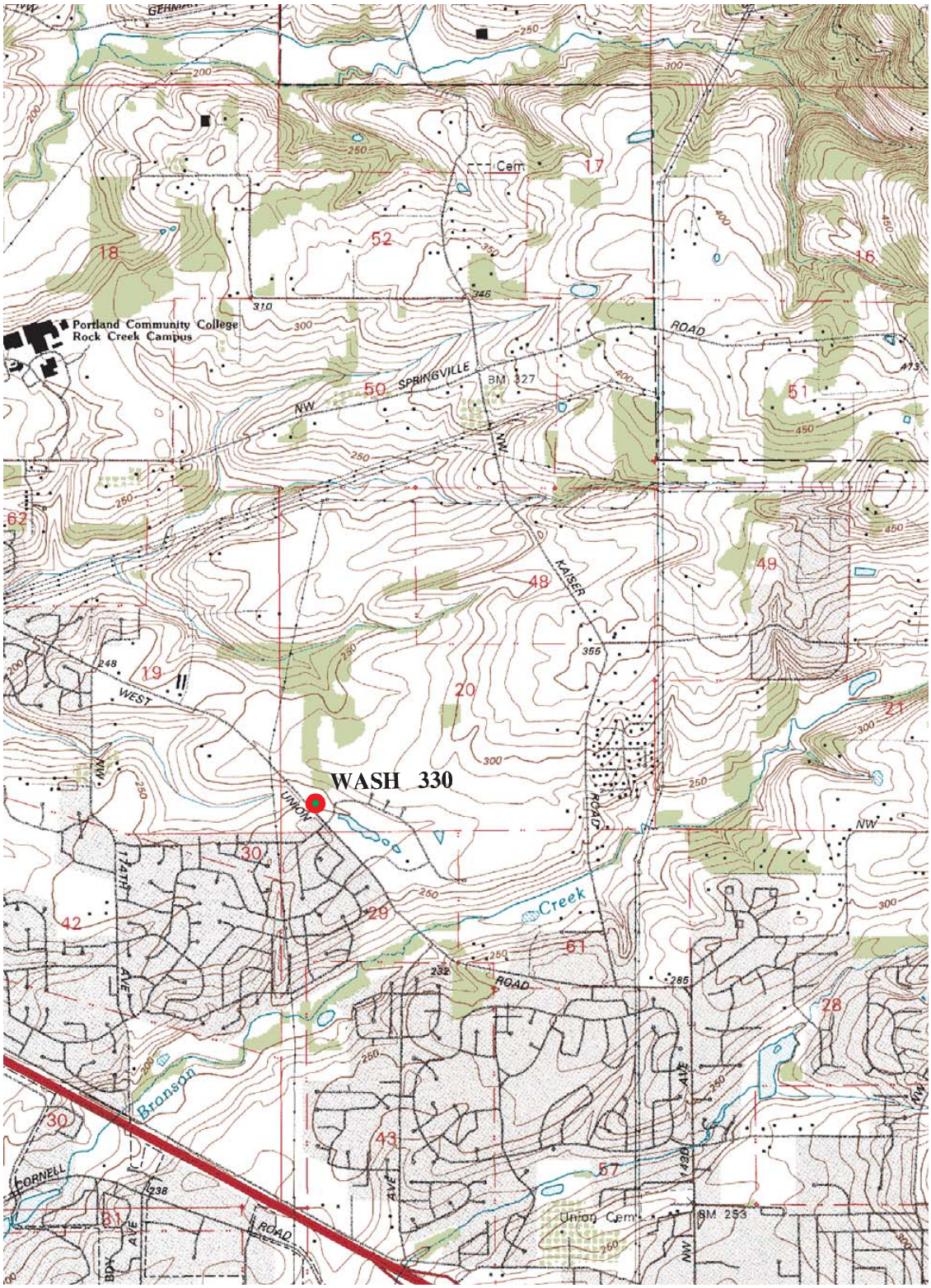

Geologic Log For Site WASH 330

NWIS Site ID: 453302122504101
OWRD Log ID: WASH 330
Well location: 01N/01W-20CCC1
Depth drilled, in feet below land surface: 1206
Land surface altitude, in feet above Nation Geodetic Vertical Datum of 1929: 246

Logged by: M. H. Beeson and T. L. Tolan
Date drilled: 06/10/1989

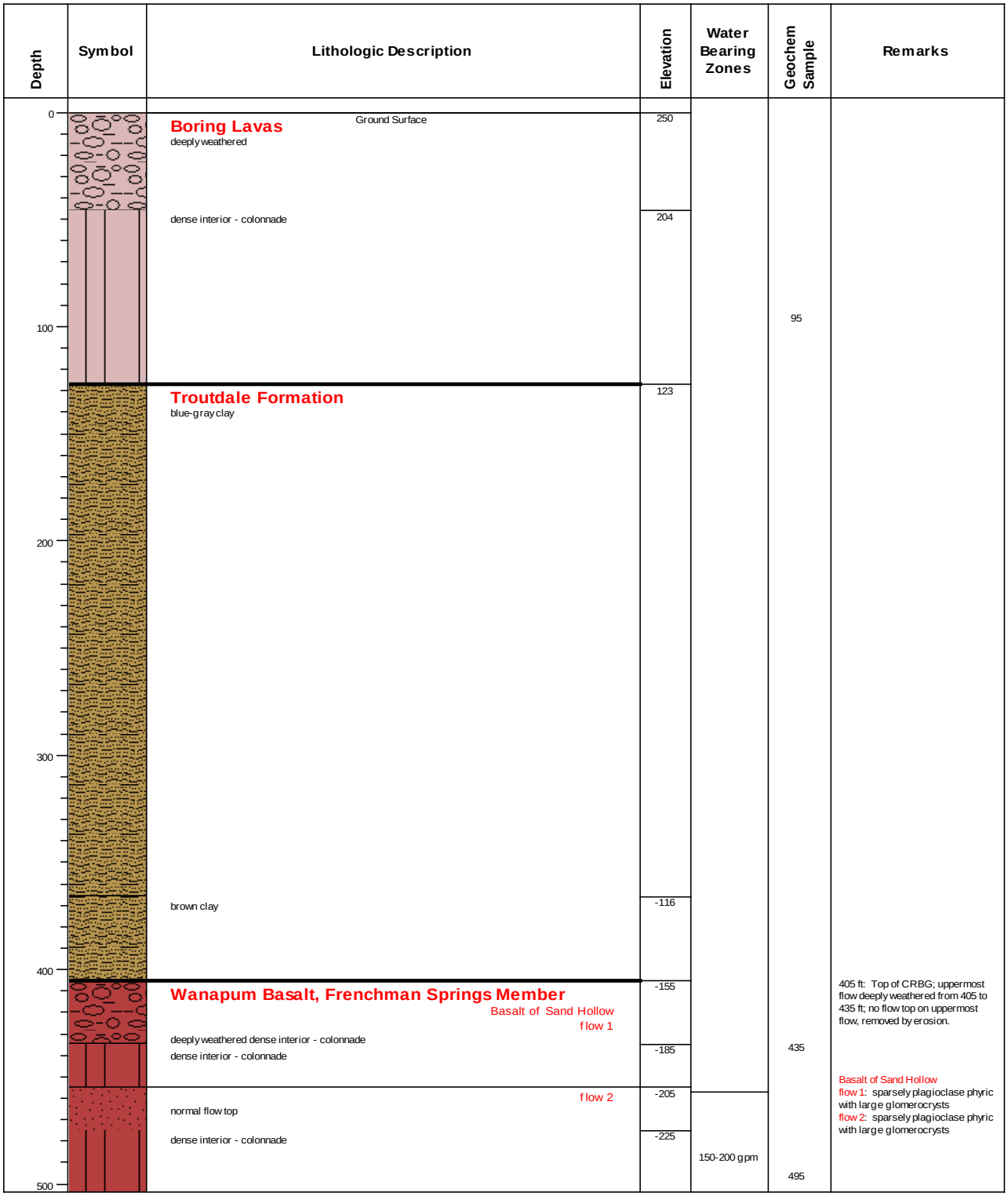

Geologic Log For Site WASH 330

NWIS Site ID: 453302122504101
OWRD Log ID: WASH 330
Well location: 01N/01W-20CCC1
Depth drilled, in feet below land surface: 1206
Land surface altitude, in feet above Nation Geodetic Vertical Datum of 1929: 246

Logged by: M. H. Beeson and T. L. Tolan
Date drilled: 06/10/1989

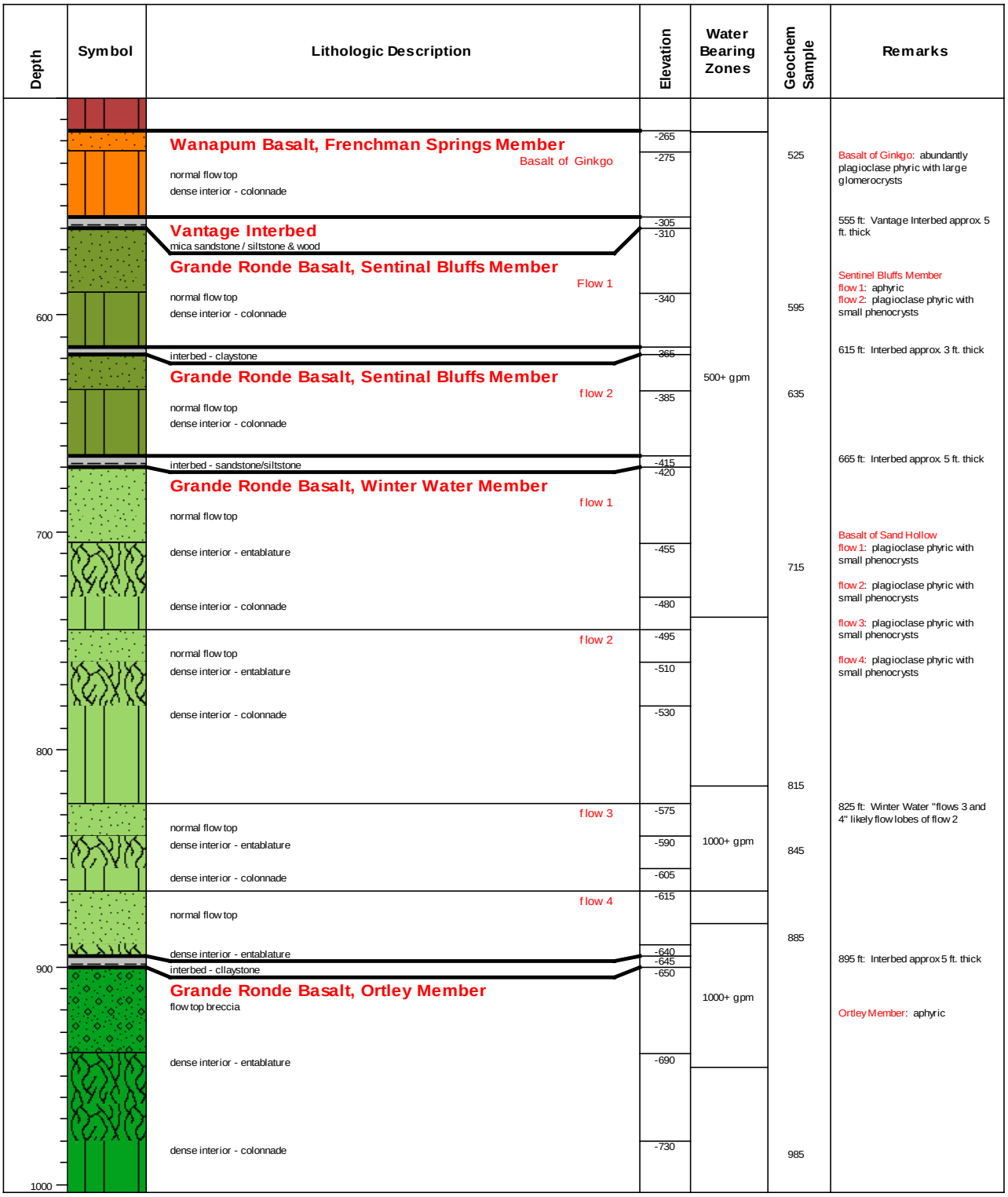

Geologic Log For Site WASH 330

NWIS Site ID: 453302122504101
OWRD Log ID: WASH 330
Well location: 01N/01W-20CCC1
Depth drilled, in feet below land surface: 1206
Land surface altitude, in feet above Nation Geodetic Vertical Datum of 1929: 246

Logged by: M. H. Beeson and T. L. Tolan
Date drilled: 06/10/1989

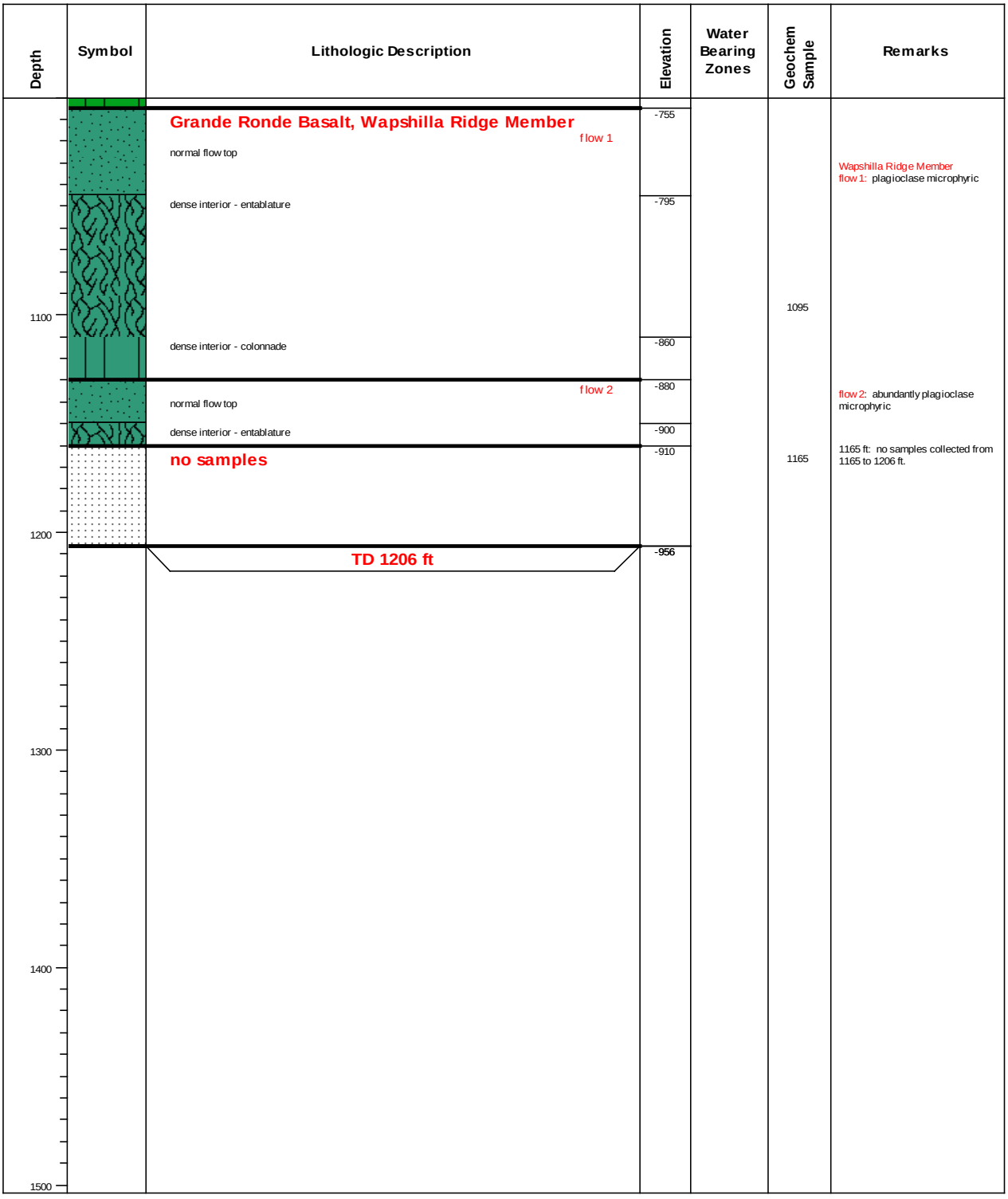

Location Map For Site WASH 886

NWIS Site ID: 453612122541301

Well location: 01N/02W-02BBD

OWRD Log ID: WASH 886

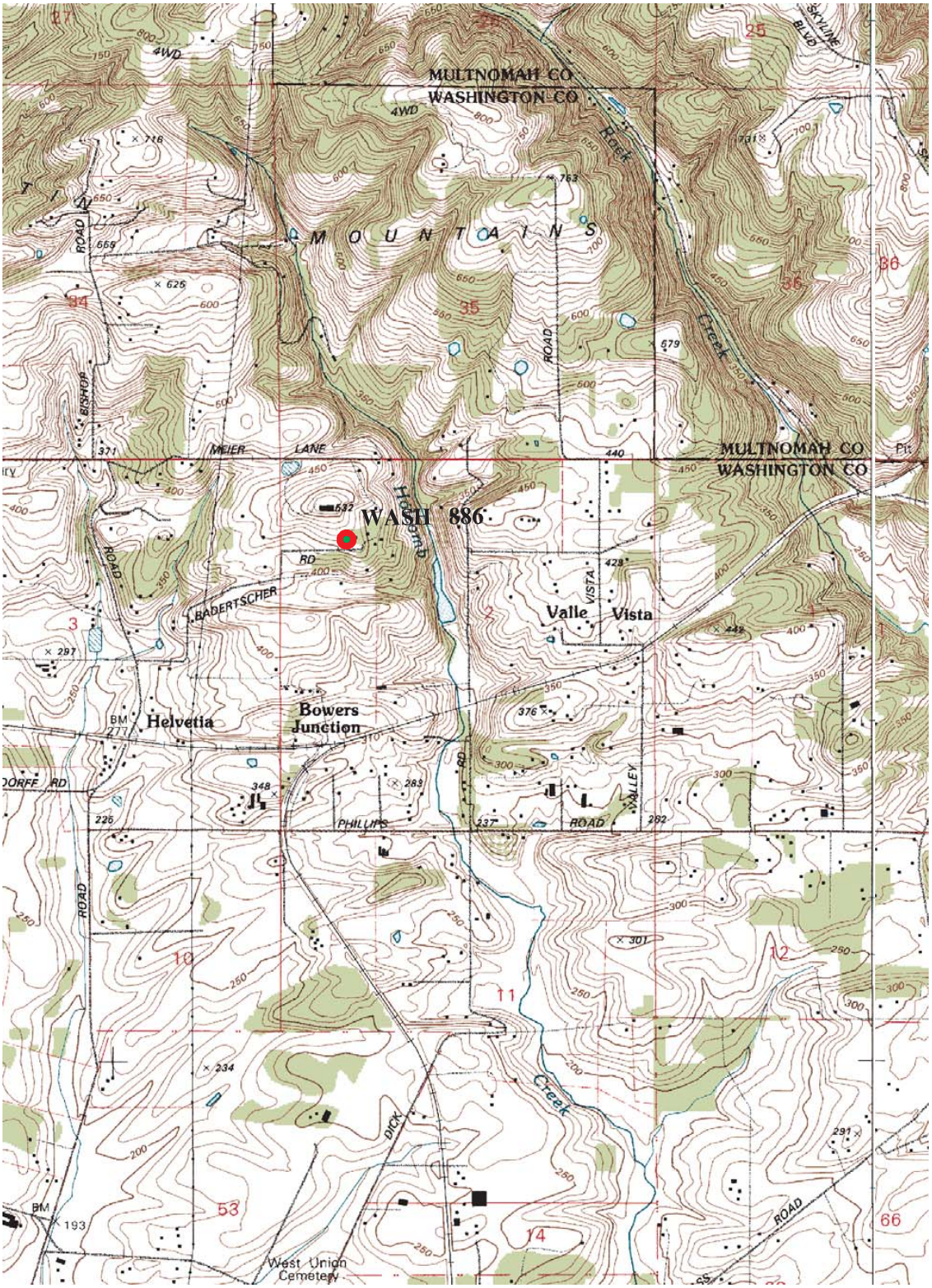

Geologic Log For Site WASH 886

NWIS Site ID: 453612122541301
OWRD Log ID: WASH 886
Well location: 01N/02W-02BBD
Depth drilled, in feet below land surface: 655
Land surface altitude, in feet above Nation Geodetic Vertical Datum of 1929: 465

Logged by: T. L. Tolan
Date drilled: 03/07/1991

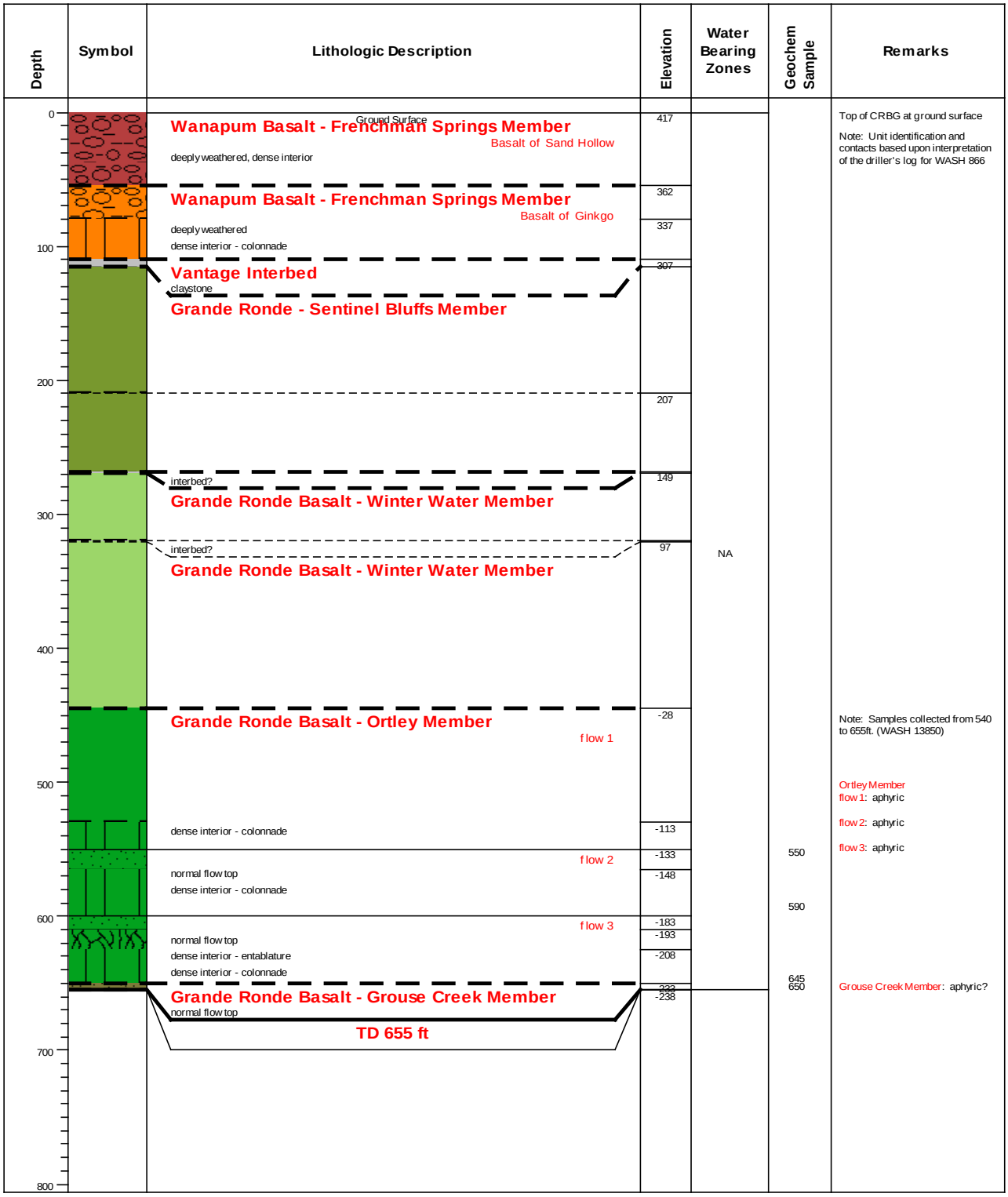

APPENDIX B: ANALYTICAL METHOD FOR WHOLE-ROCK AND TRACE ELEMENT GEOCHEMISTRY

1. 3.6000 ± 0.0002 g of lithium tetraborate are weighed out into a clean glass bottle (24 ml glass bottle from Thomas Scientific) followed by 0.4000 ± 0.0001 g of the rock powder and are mixed for 10 minutes in a Spex Mixer Mill. The homogeneous powder is transferred into a 25 cc 95% Pt-5% Au crucible, and 3 drops of a 2% solution of lithium iodide are added to the powder to reduce the viscosity of the mixture as it is heated over a Meeker burner while mounted on a standard ring stand. During heating the crucible is covered with a 95% Pt-5% Au lid, which also acts as the mold into which the molten sample will be poured and cast into a disc shape. The bottom of the Pt lid is flat and highly polished; thus, the side of the disc in contact with the Pt lid is the one exposed to the primary X-ray beam.
2. The heating period is normally 10 minutes, with the sample being vigorously stirred while holding the crucible with a pair of Pt-tipped tongs at both the 3-minute and 6-minute marks. After sufficient heating so that the molten sample is thoroughly convecting, the Pt lid is removed from the crucible with a pair of tongs and is heated over a Bunsen burner until it is red-hot. With a second pair of tongs the crucible is removed rapidly from suspension on the ring stand over the first burner and emptied onto the hot Pt lid. With some practice virtually all of the crucible's contents are transferred to the lid. Immediately upon completing the pouring event, the still hot crucible is dropped into a warm beaker containing sufficient 4N HCl to cover the crucible. With the other hand, the crucible, which has been held quite level, is now carefully placed on a flat surface; in our lab this is a flat, polished piece of granite. The sample will cool in 3 to 5 minutes so that the glass disc can be labeled with a magic marker, labeled on the side of the disc exposed to the air. The disc can be stored indefinitely in a desiccator. The major elements are determined via this technique together with Sr, Zr, Cr, and V.
3. Working curves for each element of interest are determined by analyzing geochemical rock standards, data for which have been synthesized byAbbey (1983) and Govindaraju (1994). Between 30 and 50 data points are gathered for each working curve; various elemental interferences are also taken into account, e.g., SrKß on Zr, RbKß on Y, etc. The Rh Compton peak is used for a mass absorption correction. Slope and intercept values, together with correction factors for the various wavelength interference, are calculated and then stored on a computer. A Philips 2404 X-ray fluorescence vacuum spectrometer equipped with a 102-position sample changer and a 4-kW Rh X-ray tube is used for automated data acquisition and reduction.
4. The amount of ferrous Fe is titrated using a modified Reichen and Fahey (1962) method, and loss on ignition is determined by heating an exact aliquot of the sample at 950°C for one hour. The X-ray procedure determines the total Fe content as Fe_2O_3T.
5. Trace element analysis is accomplished by weighing out 7.0000 ± 0.0004 g of whole rock powder and adding 1.4000 ± 0.0002 g of high-purity copolywax powder, mixing for 10 minutes, and pressing the sample into a briquette. Data are reported as parts per million (ppm). The elements measured this way include: Rb, Sr, Y, Zr, Nb, Ni, Ga, Cu, Zn, U, Th, Co, Pb, Sc, Cr, and V. La, Ce, and Ba have been calibrated using an L X-ray line and a mass absorption correction.
6. Please Note—always keep in mind that the original rock/mineral powder must be crushed so that ALL of the sample passes through a clean 80-mesh sieve screen. Do NOT use tungsten carbide grinding vessels if at all possible.

References

Abbey, S., 1983, Studies in "standard samples" of silicate rocks minerals 1969–1982: Geological Survey of Canada Paper 83-15, p. 1–114.

Govindaraju, K. 1994, 1994 compilation of working values and sample description for 383 geostandards: Geostandards Newsletter, v. 18, Special Issue, p. 1–158.

Reichen, L. E., and Fahey, J. J., 1962, An improved method for the determination of FeO in rocks and minerals including garnet: U.S. Geological Survey Bulletin 1144B, p. 1–5.

Additional Sources

Bennett, H., and Oliver, G., 1992, XRF analysis of ceramic, minerals and allied materials: New York, John Wiley and Sons, 298 p.

Boyd, F. R., and Mertzman, S. A., 1987, Composition of structure of the Kaapvaal lithosphere, southern Africa, *in* Mysen, B. O., ed., Magmatic processes — physicochemical principles, Special Publication 1: St. Louis, Mo., Geochemical Society, p. 13–24. [Contains description of XRF methodology]

Hower, J., 1959, Matrix corrections in the X-ray spectrographic trace element analysis of rocks and minerals: American Mineralogist, v. 44, p. 19–32.

Mertzman, S. A., 2000, K-Ar results from the southern Oregon – northern California Cascade Range: Oregon Geology, v. 62, p. 99–122.

APPENDIX C: WHOLE-ROCK AND TRACE ELEMENT GEOCHEMICAL DATA

Data in Tables C1 and C2 are also available in a Microsoft Excel spreadsheet as part of this publication.

Table C1. Linnton Quadrangle Whole-Rock Geochemical Data.

				Oxides, weight percent													
Specimen	UTM E 83	UTM N 83	Unit	SiO_2	TiO_2	Al_2O_3	Fe_2O_3	FeO	MnO	MgO	CaO	Na_2O	K_2O	P_2O_5	LOI	Total	Fe_2O_3T	FeOT
QV01-31	519381	5039686	Qbep	53.48	1.326	17.57	0.00	7.93	0.133	5.90	7.85	3.70	0.79	0.335	0.00	99.02	0.00	0.00
QV01-32	518641	5039592	Qbep	53.36	1.343	17.02	0.00	8.07	0.134	5.69	7.92	3.78	1.00	0.340	0.00	98.66	0.00	0.00
QV01-33	519304	5039225	Qbep	54.11	1.312	17.16	0.00	7.75	0.133	5.80	7.74	3.86	0.96	0.327	0.00	99.15	0.00	0.00
781+84	519249	5039222	Qbep	54.17	1.342	16.79	0.00	8.75	0.139	6.15	7.32	3.92	1.04	0.292	0.00	99.92	0.00	0.00
92TB-14	519171	5039205	Qbep	54.28	1.299	17.01	0.00	8.07	0.136	6.02	7.80	3.91	0.97	0.323	0.00	99.82	0.00	0.00
QV03-127	518089	5039281	Qbep	53.79	1.334	17.14	0.00	8.22	0.135	5.70	7.92	3.85	1.02	0.335	0.00	99.44	0.00	0.00
QV03-129	516722	5040630	Qcmc	52.97	1.322	18.24	0.00	8.27	0.144	6.12	8.07	3.95	0.83	0.302	0.00	100.21	0.00	0.00
QV01-45	515575	5039838	Qcmc	53.26	1.368	17.39	0.00	8.04	0.137	5.80	8.06	3.73	0.92	0.336	0.00	99.04	0.00	0.00
PDX-1400	518650	5039584	Qtb	52.75	1.350	17.01	2.56	6.00	0.140	5.82	7.92	3.64	0.91	0.350	1.08	99.53	9.23	8.31
PDX-1401	519091	5040046	Qtb	53.72	1.300	16.50	3.27	5.18	0.130	5.79	7.69	3.48	0.93	0.370	1.86	100.22	9.03	8.13
PDX-1402	519328	5039537	Qtb	52.09	1.310	17.35	3.88	4.89	0.140	6.20	7.76	3.47	0.72	0.330	1.82	99.96	9.31	8.38
QV03-182	514948	5044123	Qcmc	53.21	1.305	17.77	0.00	7.98	0.139	5.88	8.20	3.94	0.88	0.302	0.00	99.60	0.00	0.00
QV03-107	515666	5041489	Qcmc	53.49	1.316	18.27	0.00	8.04	0.155	5.82	7.58	3.90	0.91	0.315	0.00	99.81	0.00	0.00
PDX-1412	513076	5045119	Qbkr	48.60	2.030	15.94	4.89	5.76	0.150	8.02	8.33	3.09	1.22	0.390	1.81	100.23	11.29	10.16
QV01-34	513076	5045119	Qbkr	49.72	2.058	15.95	0.00	9.77	0.163	7.58	8.97	3.29	1.27	0.395	0.00	99.17	0.00	0.00
PDX-1257	516678	5039926	QTb	54.00	1.430	17.20	4.79	4.07	0.140	5.19	7.72	3.67	1.11	0.400	0.63	100.35	9.31	8.38
QV03-138	515791	5040432	Qbst	53.43	1.468	17.40	0.00	8.40	0.137	5.51	8.05	3.94	1.09	0.396	0.00	99.83	0.00	0.00
QV01-44	516681	5039900	Qbst	53.76	1.473	17.17	0.00	8.37	0.134	5.22	7.88	3.96	1.14	0.398	0.00	99.51	0.00	0.00
QV03-128	519098	5040055	Qbst	53.12	1.498	17.58	0.00	8.36	0.136	5.57	8.27	3.88	1.07	0.406	0.00	99.88	0.00	0.00
Barber-660	518121	5044628	Tggc?	54.43	2.030	14.09	1.87	9.89	0.200	3.66	7.19	2.95	1.88	0.350	1.42	99.96	12.86	11.57
Barber-720	518121	5044628	Tggc?	53.72	2.050	14.82	3.37	8.48	0.180	3.33	6.76	3.00	1.73	0.350	2.33	100.12	12.79	11.51
PDX-LM28	514212	5051262	Tgo	58.71	1.860	14.67	3.06	5.77	0.150	3.19	6.91	3.03	1.96	0.320	2.24	101.87	9.47	8.52
Barber-570	518121	5044628	Tgo	54.14	1.900	15.11	4.60	5.50	0.130	3.33	6.98	3.19	1.41	0.310	3.49	100.09	10.71	9.64
Barber-550	518121	5044628	Tgo	53.96	1.900	14.02	3.43	8.23	0.190	3.65	7.33	2.98	1.60	0.320	2.33	99.94	12.58	11.32
MULT-84713-420	511682	5049297	Tgo	55.34	1.930	13.79	1.64	10.05	0.190	3.51	7.03	3.05	1.72	0.330	1.68	100.26	12.81	11.53
Barber-600	518121	5044628	Tgo	54.01	1.960	14.31	3.61	8.21	0.180	3.56	7.03	2.80	1.67	0.310	2.48	100.13	12.73	11.45
MULT-84713-520	511682	5049297	Tgo	53.63	2.010	13.60	6.37	6.21	0.180	3.56	7.15	2.67	1.51	0.360	2.89	100.14	13.27	11.94
PDX-1260A	517167	5043941	Tgo?	57.15	1.910	14.07	2.33	6.72	0.180	3.44	6.95	2.97	1.96	0.360	1.87	99.91	9.80	8.82
PDX-1260B	517167	5043941	Tgo?	55.45	1.910	14.96	4.10	5.31	0.150	3.46	6.75	2.89	1.48	0.330	3.23	100.02	10.00	9.00
PDX-LM49	516851	5047506	Tgsb	44.83	2.440	16.60	8.22	5.61	0.150	3.84	5.63	1.68	0.57	0.350	9.92	99.84	14.45	13.00
PDX-LM52	517706	5047050	Tgsb	52.43	1.920	13.97	4.19	8.25	0.200	4.34	8.53	2.76	1.11	0.320	2.25	100.27	13.36	12.02
PDX-1211	515751	5047996	Tgsb	54.68	1.950	15.03	2.33	6.70	0.160	4.25	8.78	2.83	1.17	0.330	1.89	100.10	9.78	8.80
PDX-1264	511151	5049857	Tgsb	51.15	1.810	13.62	4.91	7.66	0.190	4.62	8.56	2.49	0.83	0.300	3.93	100.07	13.42	12.08
PDX-1314	515477	5050739	Tgsb	52.97	1.940	13.68	3.93	7.89	0.190	4.47	8.60	2.70	1.15	0.330	2.45	100.30	12.70	11.43
PDX-1317	515845	5050200	Tgsb	52.68	1.910	13.91	4.28	7.65	0.180	4.53	8.67	2.70	1.02	0.320	2.17	100.02	12.78	11.50
PDX-1335	518517	5045788	Tgsb	53.63	2.010	14.61	3.39	7.14	0.190	3.93	8.84	2.97	1.20	0.350	1.80	100.06	11.33	10.19
PDX-1337	518613	5046464	Tgsb	54.47	1.900	15.19	1.60	6.91	0.180	4.30	8.91	3.09	1.03	0.310	2.28	100.17	9.28	8.35
PDX-1350	511944	5049896	Tgsb	53.02	1.930	13.87	2.05	9.66	0.230	4.94	8.36	2.85	1.08	0.310	2.21	100.51	12.79	11.51
PDX-1351C	511958	5049693	Tgsb	52.50	1.990	13.94	4.69	6.98	0.170	3.91	8.45	2.72	1.04	0.330	3.47	100.19	12.45	11.20
PDX-1365C	512199	5050837	Tgsb	53.90	2.100	15.44	3.18	6.05	0.150	4.07	8.59	3.04	1.28	0.350	2.03	100.18	9.90	8.91
PDX-1366	511696	5051289	Tgsb	53.19	1.930	14.32	1.71	9.64	0.220	4.67	8.77	2.91	1.10	0.310	1.23	100.00	12.42	11.18
PDX-1407	510952	5051112	Tgsb	53.54	1.980	13.94	1.64	9.70	0.200	4.55	8.79	2.83	1.33	0.340	1.14	99.98	12.42	11.18
PDX-1408	510931	5051113	Tgsb	54.91	2.020	14.67	2.00	6.98	0.170	4.47	8.98	3.09	1.22	0.320	1.29	100.12	9.76	8.78

Coordinates (E, easting; N, northing) are given in Universal Transverse Mercator projection, 1983 North American datum, meter units.

LOI is loss on ignition adjusted for Fe oxidation. T is total.

Table C1 continued on page 34

Table C2. Linnton Quadrangle Trace Element Geochemical Data.

				Trace Elements, parts per million																		
Specimen	**UTM E 83**	**UTM N 83**	**Unit**	**Rb**	**Sr**	**Y**	**Zr**	**V**	**Ni**	**Cr**	**Nb**	**Ga**	**Cu**	**Zn**	**Co**	**Ba**	**La**	**Ce**	**U**	**Th**	**Sc**	**Pb**
QV01-31	519381	5039686	Qbep	7	770	19	149	142	115	166	11	23	49	92	0	324	24	28	—	1	23	3
QV01-32	518641	5039592	Qbep	9	828	20	149	146	105	153	9	19	57	92	0	357	27	59	—	0	21	3
QV01-33	519304	5039225	Qbep	9	758	20	144	150	112	166	10	21	39	94	0	342	9	38	—	4	20	4
781+84	519249	5039222	Qbep	10	749	20	150	160	128	194	10	22	70	104	0	355	18	48	—	0	30	8
92TB-14	519171	5039205	Qbep	8	771	19	144	142	126	182	10	21	79	109	0	318	5	41	—	2	17	11
QV03-127	518089	5039281	Qbep	11	864	20	150	143	117	169	10	20	53	97	0	354	20	45	—	2	20	7
QV03-129	516722	5040630	Qcmc	6	714	23	140	169	112	174	10	22	52	84	0	364	19	43	—	2	25	5
QV01-45	515575	5039838	Qcmc	8	852	21	149	150	106	161	11	24	64	93	0	363	25	59	—	2	17	4
PDX-1400	518650	5039584	Qtb	8	902	22	164	167	106	154	12	23	64	100	34	420	17	49	<0.5	1	22	4
PDX-1401	519091	5040046	Qtb	8	823	24	156	155	114	161	12	21	41	99	31	379	19	42	<0.5	2	19	5
PDX-1402	519328	5039537	Qtb	7	805	21	155	155	127	187	11	22	51	98	34	377	17	43	<0.5	2	21	4
QV03-182	514948	5044123	Qcmc	9	748	24	141	167	109	166	11	21	55	83	0	331	17	41	—	2	25	3
QV03-107	515666	5041489	Qcmc	7	703	26	146	170	149	188	11	20	69	99	0	459	30	47	—	1	24	7
PDX-1412	513076	5045119	Qbkr	18	662	26	175	221	162	310	30	21	38	88	44	485	19	50	<0.5	2	24	2
QV01-34	513076	5045119	Qbkr	18	695	23	169	212	154	295	30	19	49	87	0	389	36	51	—	5	27	1
PDX-1257	516678	5039926	QTb	10	1000	20	180	165	91	114	11	22	57	95	32	495	18	52	<0.5	2	20	6
QV03-138	515791	5040432	Qbst	10	1024	19	156	163	103	144	10	23	64	103	0	453	21	58	—	2	20	6
QV01-44	516681	5039900	Qbst	7	976	20	158	177	94	133	10	19	37	93	0	426	13	54	—	1	23	4
QV03-128	519098	5040055	Qbst	10	1086	19	158	157	94	135	10	21	60	101	0	459	23	60	—	2	20	6
Barber-660	518121	5044628	Tggc?	0	325	0	179	343	—	0	0	0	—	0	0	0	0	0	—	0	0	0
Barber-720	518121	5044628	Tggc?	0	316	0	176	348	—	0	0	0	—	0	0	0	0	0	—	0	0	0
PDX-LM28	514212	5051262	Tgo	59	343	42	189	297	10	21	14	24	23	147	34	1350	22	65	2.5	6	27	9
Barber-570	518121	5044628	Tgo	0	352	0	190	308	—	0	0	0	—	0	0	0	0	0	—	0	0	0
Barber-550	518121	5044628	Tgo	0	340	0	180	315	—	0	0	0	—	0	0	0	0	0	—	0	0	0
MULT-84713-420	511682	5049297	Tgo	54	335	39	184	293	12	17	14	24	29	144	44	646	22	52	1.2	7	31	8
Barber-600	518121	5044628	Tgo	0	324	0	173	326	—	0	0	0	—	0	0	0	0	0	—	0	0	0
MULT-84713-520	511682	5049297	Tgo	52	337	39	176	342	15	29	13	23	20	146	41	641	18	50	1.9	6	31	8
PDX-1260A	517167	5043941	Tgo?	56	311	43	213	297	7	18	13	23	15	129	38	1015	21	57	2.1	6	28	8
PDX-1260B	517167	5043941	Tgo?	45	317	39	200	291	11	28	13	24	27	137	37	847	22	54	2.1	6	34	7
PDX-LM49	516851	5047506	Tgsb	4	183	28	182	273	33	37	14	28	47	124	40	772	22	43	<0.5	3	41	8
PDX-LM52	517706	5047050	Tgsb	30	327	40	157	320	18	47	13	23	40	141	37	455	16	40	1.1	4	34	7
PDX-1211	515751	5047996	Tgsb	27	314	45	183	330	13	44	12	23	34	139	44	659	24	35	1.8	4	37	6
PDX-1264	511151	5049857	Tgsb	22	303	39	158	306	17	46	11	22	32	114	40	440	19	33	0.8	4	34	6
PDX-1314	515477	5050739	Tgsb	27	311	37	165	312	20	42	12	21	25	129	49	490	16	45	1.1	4	33	7
PDX-1317	515845	5050200	Tgsb	24	315	35	162	316	21	46	12	21	24	133	45	611	17	43	1.5	6	35	7
PDX-1335	518517	5045788	Tgsb	31	334	39	166	322	20	61	13	22	25	142	43	667	17	39	<0.5	6	38	7
PDX-1337	518613	5046464	Tgsb	24	339	37	179	363	42	50	12	23	25	131	60	700	15	45	0.8	4	35	8
PDX-1350	511944	5049896	Tgsb	28	305	38	163	309	12	48	12	22	23	130	43	531	17	48	<0.5	5	32	7
PDX-1351C	511958	5049693	Tgsb	29	318	37	170	340	12	43	12	22	23	135	40	495	17	45	2.6	5	39	7
PDX-1365C	512199	5050837	Tgsb	31	340	50	187	330	8	41	12	23	29	149	35	746	22	54	0.6	4	36	7
PDX-1366	511696	5051289	Tgsb	28	315	37	164	322	15	45	12	22	25	143	44	531	17	47	0.7	3	31	7
PDX-1407	510952	5051112	Tgsb	32	327	38	173	327	14	48	13	23	24	131	43	515	17	39	1.4	4	32	4
PDX-1408	510931	5051113	Tgsb	31	353	46	179	330	12	51	13	24	38	143	36	615	17	47	<0.5	4	35	5

Coordinates (E, easting; N, northing) are given in Universal Transverse Mercator projection, 1983 North American datum, meter units.
LOI is loss on ignition adjusted for Fe oxidation. T is total.

Table C2 continued on page 35

Table C1 continued from page 32

				Oxides, weight percent													
Specimen	**UTM E 83**	**UTM N 83**	**Unit**	**SiO_2**	**TiO_2**	**Al_2O_3**	**Fe_2O_3**	**FeO**	**MnO**	**MgO**	**CaO**	**Na_2O**	**K_2O**	**P_2O_5**	**LOI**	**Total**	**Fe_2O_3T**	**FeOT**
PDX-1409	510805	5050758	Tgsb	55.45	2.080	14.86	2.17	6.10	0.160	4.25	8.76	3.12	1.27	0.350	1.77	100.34	8.95	8.05
PDX-LM73	519265	5044419	Tgsb	51.94	1.970	14.00	4.30	8.14	0.200	4.37	8.78	2.68	1.04	0.330	2.33	100.08	13.35	12.01
PDX-LM2	517643	5048219	Tgww	55.65	2.050	13.26	2.50	9.91	0.210	3.27	6.79	2.91	1.85	0.390	1.57	100.36	13.51	12.16
PDX-LM61	516735	5047580	Tgww	54.57	2.130	14.08	5.58	5.21	0.160	3.08	6.61	2.95	1.91	0.380	3.41	100.07	11.37	10.23
Barber-440	518121	5044628	Tgww	54.68	2.080	13.55	2.84	9.74	0.200	3.42	6.99	3.07	1.64	0.350	1.45	100.01	13.66	12.29
Barber-490	518121	5044628	Tgww	54.18	1.980	14.06	3.28	8.56	0.190	3.56	7.20	3.01	1.64	0.340	1.98	99.98	12.79	11.51
Barber-520	518121	5044628	Tgww	54.29	2.030	14.66	3.11	7.99	0.200	3.63	7.24	2.88	1.77	0.360	2.06	100.22	11.99	10.79
PDX-1193	516343	5050136	Tgww	55.38	2.050	13.42	2.38	9.93	0.210	3.29	6.78	2.90	1.85	0.380	1.46	100.03	13.42	12.08
MULT-84713-300	511682	5049297	Tgww	55.23	2.100	13.47	3.22	8.68	0.190	3.20	6.75	3.16	1.80	0.370	1.73	99.90	12.87	11.58
PDX-1307	514647	5050052	Tgww	57.09	2.190	14.62	2.91	5.34	0.150	3.06	6.87	3.13	2.17	0.390	2.28	100.20	8.84	7.95
PDX-1195	516521	5049800	Tgww	55.81	2.020	12.95	2.83	9.17	0.190	3.15	6.76	2.91	1.94	0.360	1.31	99.40	13.02	11.72
PDX-1303	514676	5050082	Tgww	56.36	2.070	13.85	2.16	7.86	0.200	3.31	7.06	2.92	2.06	0.370	1.76	99.98	10.90	9.81
PDX-1305	514761	5049785	Tgww	55.38	2.140	14.38	4.45	5.39	0.150	3.21	6.96	3.08	1.74	0.350	2.73	99.96	10.44	9.39
PDX-1360	510826	5051150	Tgww	56.23	2.110	13.91	2.51	7.59	0.190	3.37	7.01	3.12	2.03	0.380	1.37	99.82	10.95	9.85
PDX-1261	516535	5044109	Tgww	54.07	2.070	12.89	6.39	7.15	0.200	3.13	6.69	2.84	1.57	0.370	2.98	100.35	14.34	12.90
PDX-1403	517479	5043969	Tgww	55.84	2.140	13.56	1.98	8.78	0.210	3.50	7.12	3.03	1.80	0.380	1.75	100.09	11.74	10.56
PDX-1405	510859	5051127	Tgww	56.09	2.080	13.75	2.78	8.18	0.200	3.36	7.08	3.04	1.99	0.370	1.50	100.42	11.87	10.68
PDX-1422	512598	5052298	Tgww	54.02	2.110	14.28	4.64	5.98	0.160	3.44	7.18	2.95	1.46	0.330	3.68	100.23	11.29	10.16
PDX-LM7	516511	5048201	Tgww?	57.34	2.140	14.30	2.33	6.45	0.180	3.07	6.74	3.12	2.09	0.400	1.79	99.95	9.50	8.55
PDX-1263	513806	5048055	Tgww?	55.84	2.220	14.66	3.18	6.46	0.180	3.17	6.74	3.11	1.79	0.400	2.13	99.88	10.36	9.32
PDX-1265	514346	5047553	Tgww?	56.25	2.090	13.58	2.39	8.32	0.200	3.25	6.85	3.01	1.81	0.390	1.85	99.99	11.64	10.47
PDX-1196	516450	5049764	Tgwwh	55.01	1.980	13.55	2.15	10.04	0.210	3.86	7.60	2.82	1.56	0.330	1.26	100.37	13.31	11.98
PDX-LM17	515022	5051616	Tgwwh	55.34	2.040	13.93	1.87	9.18	0.200	3.91	7.74	3.08	1.53	0.310	1.11	100.24	12.07	10.86
PDX-1196	516450	5049764	Tgwwh	54.10	2.010	13.42	2.05	10.42	0.200	3.93	7.64	2.82	1.58	0.310	1.52	100.00	13.63	12.26
PDX-1198	518405	5047335	Tgwwh	54.45	2.030	13.52	3.27	9.33	0.190	3.71	7.20	3.10	1.43	0.330	1.57	100.13	13.64	12.27
PDX-1346	518499	5046754	Tgwwh	55.56	2.070	14.35	2.10	7.85	0.190	3.76	7.82	3.33	1.44	0.320	1.18	99.97	10.82	9.74
PDX-LM3	517455	5048345	Tgwwh	55.33	2.010	13.74	2.27	9.16	0.210	3.70	7.39	2.95	1.59	0.350	1.32	100.02	12.45	11.20
PDX-1406	510902	5051152	Tgwwh	55.54	2.080	14.59	2.28	7.06	0.180	3.84	7.95	3.23	1.62	0.320	1.31	100.00	10.13	9.12
W97-36	509845	5050282	Tgww	56.07	2.169	13.83	0.00	11.07	0.196	3.52	7.51	3.11	1.60	0.352	0.00	99.43	0.00	0.00
W97-37	509845	5050282	Tgsb	54.39	2.049	14.47	0.00	10.44	0.173	4.28	8.70	2.89	1.20	0.340	0.00	98.93	0.00	0.00
PDX-232	515054	5045042	Tfsh	48.77	2.990	13.48	6.88	7.23	0.420	3.22	8.63	2.59	0.84	0.590	4.14	99.78	14.92	13.43

Coordinates (E, easting; N, northing) are given in Universal Transverse Mercator projection, 1983 North American datum, meter units.

LOI is loss on ignition adjusted for Fe oxidation. T is total.

Table C2 continued from page 33

				Trace Elements, parts per million																	
Specimen	**UTM E 83**	**UTM N 83**	**Unit**	**Rb**	**Sr**	**Y**	**Zr**	**V**	**Ni**	**Cr**	**Nb**	**Ga**	**Cu**	**Zn**	**Co**	**Ba**	**La**	**Ce**	**U**	**Th**	**Sc**	**Pb**
PDX-1409	510805	5050758	Tgsb	33	361	42	185	345	19	47	13	24	33	141	42	1510	17	54	1.2	4	35	3
PDX-LM73	519265	5044419	Tgsb	28	324	39	170	334	10	53	13	23	26	131	40	429	17	44	<0.5	6	35	4
PDX-LM2	517643	5048219	Tgww	54	294	38	207	321	6	21	13	23	18	131	39	661	18	54	1.4	6	27	7
PDX-LM61	516735	5047580	Tgww	58	349	47	189	316	8	19	15	25	16	157	41	869	21	55	1.7	6	31	9
Barber-440	518121	5044628	Tgww	0	326	0	178	351	—	0	0	0	—	0	0	0	0	0	—	0	0	0
Barber-490	518121	5044628	Tgww	0	341	0	183	319	—	0	0	0	—	0	0	0	0	0	—	0	0	0
Barber-520	518121	5044628	Tgww	0	333	0	182	354	—	0	0	0	—	0	0	0	0	0	—	0	0	0
PDX-1193	516343	5050136	Tgww	54	293	38	204	312	6	18	13	23	13	133	40	664	20	42	2	7	29	7
MULT-84713-300	511682	5049297	Tgww	56	329	41	209	323	9	19	15	25	13	152	42	656	19	56	0.9	5	31	9
PDX-1307	514647	5050052	Tgww	61	355	48	217	353	3	18	14	24	5	157	42	1035	20	71	2.6	8	30	9
PDX-1195	516521	5049800	Tgww	59	318	39	194	316	4	20	14	22	4	143	40	659	21	55	1.4	11	29	9
PDX-1303	514676	5050082	Tgww	58	329	42	204	340	4	19	14	24	5	150	44	801	20	62	2.6	7	29	9
PDX-1305	514761	5049785	Tgww	50	341	48	199	361	3	21	13	23	7	145	38	921	21	68	1.7	7	33	9
PDX-1360	510826	5051150	Tgww	59	332	43	209	342	4	22	13	24	4	153	39	1025	19	67	1	8	27	8
PDX-1261	516535	5044109	Tgww	47	328	38	196	327	7	21	14	24	3	127	39	812	22	47	1.9	9	27	5
PDX-1403	517479	5043969	Tgww	54	336	45	204	353	4	21	15	24	4	150	40	725	20	56	1.5	7	29	6
PDX-1405	510859	5051127	Tgww	56	338	40	205	351	3	20	15	24	2	141	39	695	23	53	1.8	7	28	6
PDX-1422	512598	5052298	Tgww	41	350	47	208	373	4	21	13	24	9	160	35	817	23	51	<0.5	4	33	6
PDX-LM7	516511	5048201	Tgww?	58	328	44	235	326	6	17	14	25	8	148	38	905	22	76	2.5	7	27	8
PDX-1263	513806	5048055	Tgww?	50	319	45	237	322	5	20	14	25	15	144	35	1003	23	65	2.1	8	30	8
PDX-1265	514346	5047553	Tgww?	53	310	42	214	320	6	19	14	23	11	140	36	823	20	61	2.5	9	32	8
PDX-1196	516450	5049764	Tgwwh	43	297	36	187	350	8	22	13	23	17	128	46	575	17	46	2.1	5	32	7
PDX-LM17	515022	5051616	Tgwwh	45	323	38	184	371	5	25	12	23	10	144	40	640	19	51	1	8	30	9
PDX-1196	516450	5049764	Tgwwh	45	322	37	177	350	6	24	13	23	8	131	41	580	19	46	<0.5	6	30	8
PDX-1198	518405	5047335	Tgwwh	43	312	37	178	359	6	22	13	23	6	137	45	600	20	48	1.8	7	30	9
PDX-1346	518499	5046754	Tgwwh	42	323	41	183	345	4	22	13	24	7	158	43	699	18	52	1	5	31	8
PDX-LM3	517455	5048345	Tgwwh	46	300	38	199	345	7	20	13	24	19	132	42	659	18	45	3.1	6	30	7
PDX-1406	510902	5051152	Tgwwh	45	361	41	196	388	5	24	14	25	6	145	41	690	17	58	1.8	4	32	5
W97-36	509845	5050282	Tgww	44	334	47	187	369	3	26	14	21	10	158	0	792	18	58	nd	5	36	10
W97-37	509845	5050282	Tgsb	26	328	36	163	334	13	53	12	23	32	124	0	529	7	46	nd	2	40	6
PDX-232	515054	5045042	Tfsh	24	329	55	190	380	22	55	16	22	34	153	41	810	0	0	1	4	37	8

Coordinates (E, easting; N, northing) are given in Universal Transverse Mercator projection, 1983 North American datum, meter units.
LOI is loss on ignition adjusted for Fe oxidation. T is total.